Author Manuscript

Author Manuscript

Author Manuscript

Author Manuscript

HHS Public Access

Author manuscript

Transplantation. Author manuscript; available in PMC 2020 July 01.

Published in final edited form as:

Transplantation. 2019 July ; 103(7): 1306–1322. doi:10.1097/TP.0000000000002656.

Enhancing the Value of Histopathological Assessment of Allograft Biopsy Monitoring

Michelle A. Wood-Trageser, PhD[1], **Andrew J. Lesniak**[1], and **Anthony J. Demetris, MD**[1]

[1]Division of Transplant Pathology, Department of Pathology, University of Pittsburgh School of Medicine, Pittsburgh, Pennsylvania, USA

Abstract

Introduction: Traditional histopathological allograft biopsy evaluation provides, within hours, diagnoses, prognostic information, and mechanistic insights into disease processes. However, proponents of an array of alternative monitoring platforms, broadly classified as “invasive” or “noninvasive” depending on whether allograft tissue is needed, question the value proposition of tissue histopathology. The authors explore the pros and cons of current analytical methods relative to the value of traditional and next generation histopathological evaluation of tissue biopsies.

Objectives: Illustrate the continuing value of traditional histopathological tissue assessment and “next generation pathology (NGP)”, broadly defined as staining/labeling techniques coupled with digital imaging and automated image analysis.

Summary: Noninvasive imaging and fluid (blood, urine) analyses promote low-risk, global organ assessment, and “molecular” data output, respectively; invasive alternatives promote objective, “mechanistic” insights by creating gene lists with variably increased/decreased expression compared to steady-state/baseline. Proponents of alternative approaches contrast their preferred methods with *traditional* histopathology that: 1) fail to cite the main value of traditional and NGP - retention of spatial and inferred temporal context available for innumerable objective analyses; and 2) belie an unfamiliarity with the impact of advances in imaging and software-guided analytics on emerging histopathology practices. Illustrative NGP examples demonstrate the value of multi-dimensional data that preserves tissue-based spatial and temporal contexts.

Conclusion: We outline a path forward for clinical NGP implementation where “software-assisted sign-out” will enable pathologists to conduct objective analyses that can be incorporated into their final reports and improve patient care.

Corresponding Author: Anthony J. Demetris, E741 UPMC Montefiore, 200 Lothrop Street, Pittsburgh, PA 15213. demetrisaj@umpc.edu.

Conflicts of interest: Authors have no conflicts to disclose.

Statement of Authorship: Contributions: MWT, AL, and AJD all contributed to writing of the manuscript, supplement, and production of figures

Author Manuscript Author Manuscript Author Manuscript Author Manuscript

INTRODUCTION

Strengths of Traditional Histopathology and Modern Alternatives

Traditional histopathology strengths and value derive primarily from its visual nature and retention of spatial and inferred temporal context at a submicron resolution level. Up to 80% of environmental stimuli are processed via visual pathways[1] and ~30%–50% of the cerebral cortex is devoted to processing visual signals.[2] When pathologists view organs at submicron resolution levels, hardwired visual dominance pathways immediately integrate inputs into legacy networks of pathophysiological insights. Pathologists can rapidly, reliably, and accurately: 1) identify rare (eg, isolated intimal arteritis, viral inclusions) and/or focal (eg, scars, lymphoid nodules, etc) events; 2) appreciate social relationships among cells (eg, lymphocytic tubulitis, capillaritis); 3) "age" tissue alterations into acute (hours to days), subacute (days to weeks), and chronic (months to years); and 4) recognize and rank order multiple insults.

Rapid conceptualization by humans/pathologists, comes at the expense of more precise quantitative abilities[3] leading to important criticisms of histopathology: conventional tissue staining combined with human-only visual analysis is semiquantitative, thus, somewhat subjective, non-mechanistic and poorly reproducible.[4–8] Humans are intrinsically built for estimation and not precise counting.[3] Other shortcomings of traditional histopathology may include: sampling errors, biopsies are invasive, risky, and an unpleasant patient experience; and granular morphological or contextual information might not be required in some circumstances.

Considerations regarding the value of liver, kidney, or heart allograft biopsy acquisition for histopathological examination are evolving. The English Oxford Dictionary defines "value" as "the regard that something is held to deserve; the importance, worth, or usefulness of something."[9] Under noncomplex clinical circumstances (eg, slowly evolving presumed single insult), the value of traditional histopathological biopsy analysis is questioned allowing newer noninvasive imaging tools and high throughput tissue, blood, and bodily fluid -omics platforms combined with software-assisted analytics to enter the diagnostic tool kit.

Advocates of newer noninvasive, imaging (reviewed in references 10-14) and fluid (eg, urine or blood[6,15–19]) analytical techniques promote safety and global organ assessment, mitigating biopsy shortcomings of riskiness, sampling errors, and undesirability of use for serial measurements.[5,8,10,13,20,21] However, noninvasive radiographic approaches: 1) produce low spatial resolution output; 2) often rely on indirect measurements (eg, liver stiffness as a surrogate of fibrosis) interfered with by non-fibrosis-related processes (eg, intraorgan congestion, inflammation, and patient obesity); and/or 3) introduce operator-dependent measurement variations (reviewed in references 10-14). Blood and fluid analyses provide no spatial context regarding intra-allograft events and only indirectly monitor allografts.

Advocates of high-throughput alternative tissue methodologies (eg, -omics platforms) promote value over traditional histopathology with respect to objectivity, data output, and

Author Manuscript Author Manuscript Author Manuscript Author Manuscript

"mechanistic" insights. Again, valuable spatial and inferred temporal contexts are destroyed while risks, patient avoidances, and sampling issues are the same as traditional biopsy analyses. Moreover, these methods use traditional histopathology for validation and often yield a narrow range of simplified single-insult diagnoses,[4,7,17,18,22–25] that may overlap (eg, BK nephropathy and TCMR).[7,17,23–25]

Complex data outputs are visually displayed for human consumption (eg, scatter plots, heatmaps, volcano plots) or reported as "gene lists" without rank ordering insults when more than one insult is present. Gene lists reported can vary by organ, circumstance, or lab.[17] Sample preparation and storage, interlaboratory assay reproducibility, and interpretive expertise distribution needs standardization, resulting in calls for centralization.[7,26] Large transplant centers will evaluate the cost-benefit ratio of waiting several days (mRNA expression arrays) vs. the relatively short (hours) turnaround time of biopsy evaluation and the ability to confidently act on results for patient management.

Nevertheless, "gene lists" derived from -omics platforms represent an advancement and provide important details that can be layered on legacy histopathology mechanistic insights.[27–41] For example: 1) transcripts during TCMR show increased leukocyte populations (eg, T, B, and NK cells, macrophages) and monocyte-macrophage-derived chemokines[17,23,33,42]; 2) endothelial cell mRNA profiles are perturbed in AMR[25,28,31,42–44]; and 3) chronic inflammation, mast cell, and immunoglobulin transcripts increase over time in kidney allografts.[7,45] How effectively non-histopathology-based platforms will adapt to clinical care complexities remains forthcoming. Will "grind and bind" -omics platforms be able to: 1) rank multiple insults, 2) recognize focal defects and rare events, 3) adapt to variations in tissue age and sex, 4) time post-transplant, 5) inform drug regimens, 6) provide location data regarding donor MHC antigen expression and 7) provide spatial interactions among various cell types?

Interstitial inflammation scoring in kidney allografts encompasses peculiarities not encountered with liver allografts. If renal interstitial inflammation is located in areas of scarring or occupies <10% of non-scarred renal cortex, a Banff "i" (inflammation) score of "i0" (no inflammation) is registered.[46] Any liver inflammation is registered as abnormal. "Non-scored" (i0) kidney lymphocytic infiltrates are undoubtedly contributing to the mRNA profile, which questions the value of correlations between kidney histopathology and mRNA expression profiles.

Roles of Traditional Histopathology

Traditional histopathological liver biopsy evaluation (within hours) provides[47,48]: 1) diagnosis(es); 2) pathophysiological processes involved in tissue injury (eg, TCMR, AMR, vascular issues); 3) a rank ordering of multiple simultaneous insults; 4) structural/architectural integrity assessment, including potentially irreversible damage; 5) guidance for therapeutic intervention; and 6) potentially excess tissue for translational research purposes. These traditional roles are based on hundreds of thousands (if not millions) of assays, validated over decades, and are widely available because of distributed expertise, and used as endpoints in clinical trials,[49–53] and included in USFDA guidelines.[54]

Author Manuscript Author Manuscript Author Manuscript Author Manuscript

Ranking multiple insults and recognizing mechanisms of tissue injury are increasingly important as noninvasive radiology tests decrease liver biopsy numbers conducted in noncomplex settings where one insult is imagined. For example, various radiographical approaches[10–14] might be adequate for serial monitoring of recurrent or de novo nonalcoholic fatty liver disease in an otherwise stable liver allograft recipient with negative DSA and autoimmune and viral hepatitis serologies. Patients with complex simultaneous insults (eg, suboptimal biliary tract drainage coexistent and TCMR with central perivenulitis) will likely be missed using radiographic monitoring alone and treatment (eg, stent placement versus augmented IS) greatly differs.

To maximize the value proposition of traditional histopathology, pathologists need to comprehensively communicate results and diagnoses for incorporation into patient management algorithms[51,55] (see Appendix S1). This approach is superior to issuance of "descriptive" reports. Granular templated, Banff-based, semiquantitative scoring of microscopic findings[51,55] (eg, portal inflammation and portal, subsinusoidal, or perivenular fibrosis scored: none: 0; minimal: 1; mild: 2; moderate: 3; and severe) standardizes EMR databases (Figure 1). Templated scoring facilitates translational research and enables "digital" queries of archival material, which can be melded with other data (eg, demographics, serology, mRNA expression arrays, urine proteomics) and subjected to analyses.[56–61] Scoring standardization via digital WSI archives facilitates proficiency training and consensus criteria development.[62] This is an important step toward NGP implementation when objective software-assisted scoring will replace semiquantitative scoring and provide data for DIA algorithm validation. Subsequent NGP "hybrid" approaches will combine human conceptualization skills and "savant-like" DIA capabilites[3,63] to produce "software-assisted sign-out".

Continued Value of Traditional Histopathology

Reasons repeatedly cited by advocates for indication and protocol liver allograft biopsies[64,65] and native liver biopsies in the context of hepatocellular carcinoma,[66] NASH,[52,67] chronic viral,[68] and autoimmune hepatitis[69] include: 1) detecting subclinical pathology[56,57,65,70–72] (reviewed in references 60, 64, 73, and 74); 2) discerning and analyzing pathological events at a micron resolution scale guiding pathophysiological insights[52,55,67]; 3) sampling organ-restricted events (inflammation, swelling, etc); 4) serving as an endpoint in management algorithms and clinical trials[49–53]; 5) providing detailed meaningful results within hours; and 6) providing tissue samples for other platforms.[56,57,65,68,70–72] Despite protestations that histopathology is "non-mechanistic," it discovers, documents, and provides initial pathophysiological insights into many disease processes.[28,36–38,41,56–58,75–78]

Recently recognized examples where liver allograft biopsy's value helped advance the field includes recognition and monitoring of: 1) acute[58,59,77,79] and indolent chronic antibody-mediated injury[57,80–83]; 2) processes facilitating IS minimization[49,60,61,84,85] (similar to those used to monitor AIH)[69,86]; and 3) regenerative medicine attempts to create and/or rehabilitate donor organs (reviewed in reference 87). Liver allograft recipient management complacency based on relatively normal liver injury tests in long-term survivors ignored

Author Manuscript Author Manuscript Author Manuscript Author Manuscript

decades-long concerning histopathological data of subclinical inflammation and indolently progressive fibrosis (reviewed in references 55, 73, 74, and 82-84). Serum DSA monitoring combined with traditional histopathological analysis showed a robust association among inflammation, fibrosis, and DSA positivity.[56,57,83] Uninflamed biopsies more often are indicative of successful IS minimization.[49,55,61,72,84,85]

Introduction to Next Generation Pathology

Alternative monitoring approaches should be measured against NGP, which can be broadly defined as the use of multiplex tissue labeling techniques coupled with digital imaging and viewing, automated DIA, and creation and utilization of archival systems (reviewed in references 88-92). NGP enhances the value equation for “histopathology” and can be aggregated with data from other monitoring platforms (Figure 1). Tissue staining can range from standard histochemical stains (eg, H&E, trichrome) to mIHC labeling of multiple (usually two to six) proteins, mRNA, and/or DNA analytes/targets. A “panel” refers to a complete set of stains on one slide, which can be analyzed for spatial relationships among analytes.

NGP increases the value equation for biopsy evaluation by: 1) replacing semiquantitative scoring with objective quantitative data extraction; 2) creating digital archives to feed ML platforms (see below); and 3) leveraging hypothesis-driven translational research results to develop robust, clinically-applicable panels for clinical utilization by a preexisting network of expert pathologists who are familiar with automated immunostaining, standardization, and quality control platforms (eg, CLIA, CAP).

NGP follows the general workflow (Figure 2, Table S1): 1) hypotheses formulation and antigen/primary antibody selection; 2) tissue preparation; 3) slide staining; 4) digital slide scanning; 5) image/stain quality assurance; 6) DIA and biostatistical summary; and 7) digital archiving.

Biopsy Procurement and Tissue Preservation

Biopsy value is only as good as the tissue obtained; best practices will ensure that biopsy value can be maximized. At most institutions, interventional radiologists conduct biopsies under ultrasound guidance using biopsy guns. After local anesthesia, the needles are advanced to the organ surface then Tru-Cut needles are triggered to automatically obtain a tissue core (recommended 16-gauge) of a specified depth/chamber depth (22 mm).

When our institution drifted from AASLD standard practice guidelines[47] of two 2.0 cm 16-gauge (16G) needle cores toward one 1.0–1.5 cm 18-gauge (18G) core the rate inadequate 18G core biopsies increased (approaching 30%), which in turn, prompted a formal study. Thinner gauge needles were originally intended to sample liver malignancies where a greater risk of bleeding exists.[93–95] Our prospective randomized study (n: 150), comparing 16G and 18G cores[96] showed: 1) no difference in pain or complications rates; 2) shorter 16G core lengths (1.7 cm vs 1.9 cm; $P<0.05$); and 3) more portal tracts in 16G cores (14 vs. 13; p=0.1). Of 18G biopsies, 29% were inadequate compared to 19% of 16G biopsies (p=0.17), despite 16G cores being significantly shorter.[97] Two recent larger studies (n: 427; n:

Author Manuscript Author Manuscript Author Manuscript Author Manuscript

194)[98,99] showed significantly higher inadequacy rates with 18G needles, but Iqbal et al[98] showed higher pain rates with 16G needles. Myers et al (n: 4275; gauge unreported) showed that 0.75% of patients experienced significant complications: 0.51% pain requiring hospital admission, 0.35% bleeding; and deaths (0.14%) occurred exclusively in cancer patients.[100] Similar results were reported in three other studies,[94,101,95] where terminal complications were restricted to cirrhotic and/or cancer patients.[94,101]

Needle gauge significantly affects tissue volume. Nicholson et al[102] compared 16G (0.7 mm) versus 18G (0.5 mm) kidney tissue core diameters. For a 2.0 cm-long biopsy, the cylinder volume formula ($\pi r^2 h$) shows that 16G cores yield double the tissue volume. FFPE tissue mRNA expression profiling can require up to three consecutive 20 μm curls[103] compared to a single 2–3 μm section for panel staining (see Appendix S2). To maximize approaches available for tissue monitoring, 16G cores should be the standard, and two cores are preferable. Quality metrics for all biopsy-obtaining specialists should address the consequences of: 1) inadequate biopsies; 2) institutional review board approval for a second core; and 3) restricted ability to conduct studies on excess tissue.

Tissue preservation CAP guidelines exist to ensure maintenance of target antigenicity for IHC-based clinical assays[104] (eg, HER2,[105,106] ER and PgR[107]). Immediate tissue snap freezing is ideal for antigen preservation but is generally outside of routine clinical workflow and improper cryopreservation leads to inferior morphology preservation for DIA (see Appendix S3). Clinical standard FFPE tissue preparation results in less quality variation and preserves morphology for DIA. Since formalin preparations (10% NBF vs. 4% paraformaldehyde) can produce analytical variability on an antigen-specific basis, a standard should be chosen.[108,109] Room temperature fixation in 10–20x tissue volume of 10% NBF for one hour/mm tissue thickness (generally 6 to 48 hours) is standard for most antigens.[110] Preservation-sensitive antigens (ex. p-AKT, p-ERK1/2) require immediate fixation; slicing large specimens facilitates proper fixative penetration[111,112] (See Appendix S2). While no official CAP guidance is available regarding specimen fixation for “molecular pathology” assays, guidelines exist for assay validation from a variety of inputs (ie, unfixed vs. fixed vs. FFPE).[113,114]

Formulation of Hypotheses and Antigen/Primary Antibody Selection

Hypothesis testing often leads to innumerable marker queries and panel combinations that can be simplified into key processes. Examples include characterization of immune infiltrates (eg, T, B, and NK cells, and monocyte/macrophage panels)[60,115]; relationships of cell types to tissue structures (eg, leukocytes to bile ducts or hepatocytes or capillaries via TBX21/GZMB/CK19/CAM5.2 or PTPRC/CD34/HLA-DPB1, respectively)[115–121]; spatial relationships among immune infiltrates (virtual immunological synapses[60]); cancer signaling pathways[118,120,121]; stereotypic responses to injury/stress (eg, endothelial and myofibroblast proliferation/activation via CD34/ACTA2/MKI67); and tolerogenic vs proinflammatory liver APCs (eg, IRF4/IRF8/LILRB2/HLA-DPB1/ITGAX). Cancer studies primarily focus on the tumor immune microenvironment – a mirror image of transplant immunology[122–126]. Since perturbed genes “travel in herds[7,45]“ and are network-linked,[127] hypothesis-driven or -omics-derived “gene lists” can inform more selective, and potentially more enlightening,

Author Manuscript Author Manuscript Author Manuscript Author Manuscript

NGP targets for study because it enables analyses of spatial relationships. New technologies combine spatial resolving capabilities of digital imaging with tissue-targeted mRNA expression analysis.[128]

Primary antibody or ISH probe selection is key to panel development success. Ideally, primary antibody candidates should have a robust publication use record in human tissues, be easily implemented clinically, and show compatible antigen retrieval characteristics with panel coanalytes. Novel antibodies may not meet this standard, but time is wasted trying to facilitate "poor-performing" antibodies are compounded during attempted panel inclusion. In our experience, ~70% of antibodies show robust FFPE tissue staining; the Human Protein Atlas is a generally reliable reference.[129–131] RTU or IVD antibodies should be considered as the starting point of clinically-targeted panel development[92] (See Table S1).

Multiplex Staining Approaches

Traditional mIHC approaches include the following (or combinations thereof): (1) simultaneous protein detection via primary antibodies from different host species; (2) sequential protein detection via primary antibodies from the same host species with interspersed blocking steps (Figure 2C); (3) sequential detection of proteins via primary antibodies from the same/different host species with antibody denaturation/elution between detection steps (Figure 2D). Targets can be localized with chromogens (eg, 3,3'-diaminobenzidine [DAB], 3-amino-9-ethylcarbazole [AEC], and alkaline phosphatase substrates[132] and/or fluorescent probes [ie, organic fluorophores, Opal Dyes, and Qdots]).

Antigen retrieval is usually required for FFPE tissues and impacts panel co-analyte selection because of potential incompatibilities (reviewed in references 133 and 134). Amplification systems (eg, biotin-avidin, tyramide, hapten-based, rolling circle, polymer-based, silver[89,135–137]) help to detect low expressing antigens or deterioration-sensitive targets. Newer methodologies, like multiplex ion beam imaging,[138,139] can detect ~100 analytes in FFPE tissues with: (1) improved signal-to-noise ratio and assay linearity; (2) elimination of spectral overlap; (3) analyte signal stability; (4) stable analyte registry; and (5) improved resolution compared to other mass-based reporter systems.[138] CODEX utilizes oligonucleotide-labelled antibodies, iteratively queried by labelled dNTPs, and visualized by standard fluorescent microscopy.[140] CODEX revealed 66 targets in frozen tissue sections and touts lack of antigen degradation during repeated deactivation.[140] Although new techniques circumvent the need for primary antibodies from unique species, we find it helpful (see Appendix S4). Protocols should be validated in a variety of tissue-specific specimens (ie, test stain targeted tissue; see Appendixes S5–S7).

Implementing mIHC fluorescence panels requires adjustments for possible spectral overlap and/or tissue autofluorescence (see Appendixes S5–S7). Complex mIHC panels may require splitting across several thin serial sections and digitally aligning serial sections. Algorithms can align WSI at regional (eg, portal tracts) and cell-based levels.[141] The latter requires more consideration, validation, and manual input to override error. Lopez et al achieved an automated registration accuracy of <50 μm[142] advocating thinner (3–4 μm) section use (see Appendix S2).

Author Manuscript Author Manuscript Author Manuscript Author Manuscript

Our initial mIHC panel development using Qdots[5,20] was based on indirect detection of primary antibodies using biotinylated secondary antibodies and streptavidin-linked Qdots (Figure 2, B and C; reviewed in reference 143). Initial Qdot advantages included: brightness, photostability, and a common excitation wavelength (acquisition speed facilitated by efficient metal halide excitation sources). Qdot shortcomings became apparent over time, including: lot number staining variation; signal quenching by a variety of commonly used IHC reagents; and background staining (especially in liver, see Appendix S7), which led to unreliable staining for some panels.[144,145] The availability of enhanced camera sensitivity led to a transition to fluorophore-conjugated TSA reagents (Figure 2D, for caveats see Appendix S8).[122,123,146,147] Heat deactivation and elution remove primary and secondary antibodies from the antigen binding site (to below detection levels) at each staining step. Fluorophores remain covalently bound to tyrosine residues near the antigen site via peroxidase activation.[123,136,148]

Automation of Multiplex Immunohistochemistry

Automation is essential to mIHC clinical implementation because it reduces human variation and errors while producing more predictable results and shorter turnaround times: week versus day(s) and is available in most clinical laboratories. We have experience with two platforms – LabVision Autostainer 360–2D (ThermoScientific) and Discovery ULTRA (Ventana Medical Systems/Roche). The LabVision is suited to avidin-biotin based detection systems but is limited compared to newer platforms (eg, Discovery ULTRA, Leica Bond III) by inabilities to: 1) deparaffinize; 2) enable individual protocolized slide heating for antigen retrieval or incubations (as needed for TSA and polymer-based detection reagents and ISH), which may shorten primary antibody incubation time; 3) prevent evaporation during lengthy incubations (>2–3 hours); and 4); enable more than one staining protocol per run. Newer platforms enable completion of mIHC four to five analyte panels in “overnight runs (8–15 hours)”. “Open” platforms allow investigators to customize their reagents in conjunction with vendor-specific reagents.

WSI Considerations

Clinical NGP imaging considerations include: 1) overall system costs (ie, money and time)[149]; 2) workflow integration; 3) WSI resolution; 4) scan time for transmitted light microscopy applications; 5) fluorescence scanning capabilities; 6) digital storage space; 7) trained personnel; 8) LIMS integration; 9) telepathology; and 10) regulatory hurdles.[150–152] Comprehensive reviews cover selection, implementation, and practical use of digital pathology systems in clinical practice or research settings.[153–155] Industry advocate groups (eg, CAP, Royal College of Pathologists) and software workflow improvements drive standardization and validation guidelines with respect to device and viewing platform calibration, maintenance, analytics, and validation cohort size,[156–158] In 2017, the USFDA granted Philips’ IntelliSite scanner approval for primary diagnostic use.[159] “Subscription-based” companies/services offer economical alternatives to a large upfront capital or personnel investments.[160,161]

Retrospective studies confirm diagnostic concordance between WSI and glass slides using the industry clinical standard of 20x WSI magnification (0.5 microns/pixel resolution).

Author Manuscript Author Manuscript Author Manuscript Author Manuscript

[162,163] Higher 40X magnification scanning (<0.25 micron/pixel resolution) is: 1) required for transplant and "inflammatory" pathology (eg, recognition of leukocyte phenotypes and glomerular basement membrane abnormalities)[164,165]; 2) supported by nearly all WSI vendors; 3) alleviates pathologist eye strain compared to 20X; and 4) yields over 95% diagnostic concordance compared to conventional light microscopy.[166]

Fluorescence WSI processes require upfront mIHC experimental design considerations such as fluorophore/imaging filter pairs with available excitation sources to reduce imaging artifacts such as photobleaching and poor signal-to-noise. Web accessible resources can assist with optimal component selection.[167] Improvements enabling routine use of fluorescence WSI, include: camera technologies,[168] fast excitation sources, wavelength separation,[169] improved axial resolution (Z-dimension) techniques (ie, confocal WSI scanners), and mechanical speed.[170] Emerging high-speed focus systems can leverage new camera technologies to shorten capture times,[171] and correlative microscopy approaches will enable comprehensive multi-modal imaging studies of tissue events.[172]

Fluorescence WSI scanners enable comprehensive software-based mIHC quantification (eg, NearCYTE[173]; Figure 3) and social relationships among cell types[60,119,174] (Figures 3 and 4). Graphical mIHC data displays can mimic flow cytometry while preserving spatial context and "tether" index populations back to tissue locations[119] (Figure 5). Brown et al demonstrated equivalence between mIHC and traditional flow cytometry for assessing lymphocyte populations.[158] A mIHC WSI enables systematic "reanalysis" of tissues as insights are gained from analytic datasets. The potential for combining fluorescence and brightfield imaging to predict tissue labeling "in silico" will extend spectral sensitivity.[175] Emergence of immune checkpoint inhibitors in cancer therapy will trigger widespread adaptation of digital imaging capabilities.

WSI quality assurance for DIA is a time-consuming, but essential, two-component process needed to eliminate: 1) scanning errors (eg, focus problems, tissue folds, etc)[176,177] and 2) inadequate staining. Scanning errors are being minimized by algorithmically incorporating color and focusing "metrics" to automatically detect problematic areas.[178,179] Staining quality assessment requires domain knowledge of expected staining patterns, which has been more difficult to automate.

Digital Imaging in Transplantation and Analytical Approaches

Digital imaging and DIA have a 25-year history in clinical translational transplantation research and enables a worldwide network of expert pathologists. Digital images have been used to evaluate the reproducibility of diagnoses and/or lesion scoring in kidney[180–182] and heart[183] allografts and C4d deposition in liver[184] and kidney[183] allografts. DIA approaches included: 1) pixel-based; 2) QH; 3) combinations of pixel-based, spatial and QH (ie, hand-crafted); and 4) ML. When compared with estimation techniques (eg, stereology), WSI-based analyses have provided results with acceptable correlation to human-generated assessment.[185,186]

Pixel-based "software recognition" of specified color(s) differences has been used to quantify: 1) fibrosis in liver,[61,187–191] kidney,[192–196] and heart[173,197] allografts with stains

Author Manuscript Author Manuscript Author Manuscript Author Manuscript

that enhance fibrous and non-fibrous tissue contrast (eg, Masson's and light-green trichrome, Picrosirius Red with/out polarization, collagen III immunostaining); 2) severity and phenotype of inflammatory infiltrates in kidney[115,198–200] and heart[201] allografts; 3) severity of steatosis in donor livers[202–205]; and 4) scoring of chronic allograft damage index[206] parameters. Results show that human semiquantitative scoring correlates with software-based DIA, but the latter is generally more reproducible - a key criticism of human-only traditional evaluations. Donor liver[202–205] steatosis severity evaluation, augmented by Oil Red O lipid staining[205], might benefit from DIA standardization because humans tend to overestimate the severity of steatosis compared to software-derived values.[203] Since pixel-based analysis is not computationally taxing, readily available devices such as smartphone cameras can be leveraged to assess semi-supervised steatosis quantification in donor liver biopsies.[207] Once digital fibrosis quantification tools are standardized, they will erode the subjective and poorly reproducible criticisms of histopathology.

Although pixel-based approaches are useful and simple, human intervention can be required, generated data can be limited, and spatial contexts are generally ignored. For example, pixel-based assessment of liver[187–190] and kidney[192,194,195,206] allograft fibrosis and kidney[115,198–200] and heart[201] inflammatory infiltrates often rely on humans either capturing and/or excluding ROI (eg, glomeruli, blood vessels, etc) or segmenting/selecting cortical tissue on WSI, which introduces subjectivity. Biopsies from architecturally normal or minimally fibrotic livers can yield a wide range of quantitative fibrosis expression because of sampling of variably-sized portal tracts; therefore, an assessment of architectural integrity is needed.[191,208,209]

QH groups similarly colored pixels into biologically relevant structures (eg, nuclei) that satisfy relevant predefined criteria (eg, shape and/or size). Preserved spatial data (eg, XY coordinates, morphological characteristics of discrete structures) requires high sensitivity and specificity detection algorithms, limiting adaptability due to routine error sources (ie, tissue artifacts or stain variation[210]). QH has been used for glomerular parameterization, [211,212] fibrosis assessment[213] and/or determining total infiltrative cell types and/or characteristics of particular cell types (Figures 5 and 6) within tissues. [60,115,118,119,121,214,215] Quantitative DIA evaluation of nephropathology protocol biopsies for interstitial fibrosis and tubular atrophy lesions has shown prognostic significance.[216] Assessment of assay reproducibility is essential for standardization and determining usefulness.

Complex DIA combines pixel-based and QH analyses into higher order relationships using rule sets to define tissue structures (eg, algorithmic detection of "virtual immunological synapses" in pediatric liver allografts distinguished among patient clusters enrolled in IS minimization trials; Figures 3 and 4).[60] Madabhushi et al discuss the concept of "hand-crafted" DIA features, or "features which can be connected to specific measurable image attributes and have some degree of interpretability."[217] They report interest in "graph-based" approaches (ie, using tessellations and other human interpretable spatial relationship metrics) to characterize image feature arrangement (eg, arrangement of nuclei).[217,218] Recognition of specific pathology patterns (eg, lymphocyte clustering; Figure 3) can correlate with downstream effects (eg, rejection).[219] Standardization of thresholding,

Author Manuscript Author Manuscript Author Manuscript Author Manuscript

deconvolution, and automated ROI selection can reduce variability in quantification compared to "human-powered" reproducibility.[220,221]

We[20,60,61,116,118–121,214] and others[90,122,222–225] utilized a combination of pixel-based and QH based techniques to analyze: 1) graft-infiltrative cells and relationships between and among them (Figure 5); 2) tumor immune microenvironments; and 3) side-by-side comparison of biopsies from the same recipient over time (Figure 6). Automated detection of tissue area, nuclear segmentation, and analyte expression/cell are performed via NearCYTE, a "hand-crafted" tissue-tethered cytometric software (Figure 5).[173] Multidimensional individual cell-based morphometric data (eg, size, shape, analyte expression pattern, XY coordinates, etc) can identify specific cell populations (Figure 5A-C), and subpopulations (Figure 5B-E) while maintaining spatial relationship with other cell types (ie, tissue-tethered cytometry[119]). Specific cell populations and interactions can be interrogated within a spatial context while retaining architectural features (eg, virtual immune synapses in portal tracts[60]). This approach can run "asynchronous" to pathology review and provide supporting diagnostic material (eg, density specific cell populations per mm^2 of area).

DIA creates a wealth of digital data including XY coordinates, color intensity, and size, and can be used to determine spatial relationships among cells (eg, Treg, NKT cells) and/or structures (eg, portal tracts, glomeruli) not readily appreciated and/or quantifiable by humans. Humans are "handicapped" when attempting to utilize multidimensional "big" data resources, because the data inputs are not readily amenable to routine representation methods for pattern detection. A subset of Artificial Intelligence: Machine Learning (ML) enables algorithms to "learn" by observation of input variables that are tied to particular outcomes. ML can then "predict" outcomes on fresh data sets,[226,227] which has the potential to eliminate human imposed constraints and biases.

ML methods are classified by algorithmic "learning" approaches to input data: supervised and unsupervised.[226,227] Supervised learning, the most common, "learns" by algorithmic mapping of training data variables to a known outcome (eg, variables that create a "formula" to give a known output).[226,227] A practical biopsy-centric application of supervised ML includes Content Based Histopathological Image Retrieval, where WSI archives are searched for image patterns (via color, texture or other measured attributes) of a chosen pathology (ie, interface hepatitis lesions or FSGS lesions in kidneys).[228,229] Modern ML can "blend" both supervised and unsupervised techniques to optimize performance.[226,227]

"Deep Learning" (DL; deep convolutional network) is a supervised ML method[226,227] that is employed successfully in the healthcare arena (eg, the IBM Watson Oncology tool; https://www.ibm.com/us-en/marketplace/ibm-watson-for-oncology). DL creates data information relationships at multiple levels, similar to humans (reviewed in reference 230), can incorporate absolute data values, and combine them with "abstractions" such as how quickly those values are changing. Benefits include higher training efficiency and leveraging of cloud-based parallel computing resources for performance (eg, nuclear classification of colon cancers to predict outcome).[231,232]

Author Manuscript Author Manuscript Author Manuscript Author Manuscript

ML techniques utilizing unsupervised learning do not rely on any predetermined labeling of training or outcome data, but instead depend on assumptions to discover patterns.[226,227] Unsupervised learning-based ML challenges include: 1) methods that are typically computationally expensive; 2) subtle pathology patterns (eg, "subclinical" rejection) are not well characterized making training and validation challenging, especially considering biopsy size and architectural variance; and 3) influence of data artifacts, such as histology or intra-laboratory specimen preparation variance.

Unsupervised approaches operate bias-free, and hold promise to unlock biological/pathological signatures (Figure 3E). Engagement and inclusion of pathologist-oriented insights in unsupervised learning processes provide unmatched value to minimize caveats[233]: 1) reducing non-specificity from "savant" DIA data algorithms (eg, training data selection to avoid histopathology artifact contribution), and 2) predictions grounded in observable and understandable facts.[234]

Regardless of the ML approach, pathology practices will inevitably evolve toward ML incorporation into the routine workflow to maximize specimen value. Practical applications will enable "probing" biological questions by incorporating causal modeling, distinguishing which variables influence the prediction process. Routine screening tasks (eg, fibrosis-based architectural distortion quantification) will be automated, promoting efficiency and decreasing prognostic variations for subtle changes. Pathology classifications will evolve to incorporate these subtleties, invisible to the human eye, to resolve diagnostic dilemmas (eg, invasive versus in situ carcinomas).

Digital Archiving

WSI scanners create "pixel" characteristic data from stained slides, leading to a requirement for scalable and cost-effective data storage (eg, our digital archives occupy 80+ TB). WSI data contains or is linked to, metadata (eg, semi-quantitatively scored parameters, demographics, serological laboratory data, -omics platform data, etc), including associative details undiscernible to humans, but informative to ML (Figure 1). Linking metadata and intra-WSI pixel data is critical to full NGP utilization and integration into the clinical workflow. Archival systems should be user friendly and support multiple data sources. Commercial scanner vendors offer image management systems, but they: 1) are often rigid and relatively closed, making it difficult to integrate with existing laboratory information systems; and 2) have considerable upfront and ongoing maintenance costs.

A WSI archive of longitudinally-obtained biopsies and associated metadata yields several benefits because it enables: 1) immediate availability of prior patient biopsies regardless of pathologist location; 2) side-by-side biopsy comparisons, special stains, and fluorescence microscopy (Figure 6); 3) lesion grading accuracy by comparing to consensus archival reference standards; 4) remote access for expert consultation; 5) immediate harvesting of electronically-defined groupings for mechanistic, translational research, and quality assurance initiatives; and 6) batch processing DIA comparisons between or among groups to test various hypotheses and for ML algorithms. For example, simply by changing selection criteria for group inclusion (eg, DSA+ versus DSA-; male versus female, etc) various WSI

Author Manuscript Author Manuscript Author Manuscript Author Manuscript

parameters (eg, portal inflammation) can be batch processed for comparison without having to rearrange and link associated metadata – even for parameters not previously evaluated.

Industry advocate groups (eg, Digital Imaging and Communications in Medicine) promote image storage formats and data exchange[235] standards that facilitate WSI exchange and interoperability.[236] Open source WSI software, image format interpretation, data collection and analysis frameworks enable high throughput algorithm execution and downstream organization.[237] The Open Microscopy Environment[238] and Digital Slide Archive[239] groups developed storage models and database systems that can represent and manage multi-dimensional WSI data. Cloud-based computing platforms are being leveraged for solutions that integrate search, storage, and DIA processing in a secure environment that can be cost-effectively deployed.[240,241]

NGP Translation Into a Clinical Transplant Pathology Workflow

Clinical translation of NGP platforms is needed to exploit its capabilities by distributing capabilities amongst a preexisting worldwide network of expert pathologists. Our core laboratory for multicenter and corporate-sponsored clinical trials transitioned more than a decade ago to an entirely digital workflow, including: complete barcode accessioning and tissue and slide tracking, WSI creation, automated WSI analyses, and archiving. This prototypical clinical setup has been successful primarily because of: 1) the relatively small daily case load (about 20 biopsy slides/day including standard and mIHC stains); 2) the relatively small size for the vast majority of specimens (liver, kidney, and heart biopsies), which translates into a “controllable” scanning real estate; 3) parallel Zeiss Axio Scan.Z1 WSI scanners; and 4) a team of domain experts devoted to each aspect of the NGP workflow.

Histochemically-stained biopsies are scanned quickly (~11 mm2 at 7 min/WSI at 40x, 0.11 μm/pixel resolution) whereas a four-antigen mIHC WSI biopsy might require 20–30 min/WSI. Larger specimens (eg, sections from failed allografts) require a lengthy scan time (179.74 mm2 at 66 min/WSI). In our experience, mIHC IF scanning may be reliably accomplished with a 20x apochromatic objective; yielding optimal balance between scan time and image quality (signal-to-noise), with a wider field providing greater context for focus determination. The value equation of creating WSI for all specimens in a routine clinical workflow is questionable at this time. All WSIs are subjected to intense, time consuming scrutiny for semiquantitative scoring, which will be replaced by objective “analytical modules” in the viewing software.

Problematic areas for clinical implementation include: 1) lack of a best-of-breed technology to address all considerations for an optimal WSI system and workflow; 2) a paucity of competent trained personnel; 3) LIMS integration issues[242], and 4) vendor-supplied WSI viewer incompatibility. Our development of a vendor-neutral web-based viewer complete with annotation and analytical capabilities addressed the last issue and eliminated user interface inefficiencies (Figure 6). Template development with WSI libraries specific to pathology scoring and studies will assist in LIMS system interface and improve standardization and expertise distribution.

Author Manuscript Author Manuscript Author Manuscript Author Manuscript

NGP penetration into routine clinical patient care has been limited and requires commitment from anatomic pathology groups and clinical staff they support (eg, surgeons, hepatologists, nephrologists). Transplant biopsies require STAT results with “hours” turnaround time for diagnostic rendering. The necessary infrastructure for obtaining and properly triaging needle biopsies already exists and includes core(s) triaged for FFPE (1.5 – 2.0 cm needle cores) and a smaller needle core segment (3–5 mm) triaged for frozen section C4d staining. Although actual pathologist slide review time via WSI is slightly increased compared to glass slides for routine biopsy stains (personal observations and references 180 and 182), the time cost of implementing digital imaging for routine semiquantitative evaluation would currently not exceed two hours. Overnight mIHC staining and quantitative DIA would necessitate that NGP-derived data would require one to two days for more detailed objective data output (eg, pathogenic mechanisms, detailed assessments of the microvasculature.[173] fibrosis, other architectural distortions).

Developmental arms of clinical immunostaining laboratories will be responsible for panel development, similar to the current workflow. Once validated, panel staining automation and QA by trained laboratory personnel can be implemented with overnight turnaround times for as many as four to five protein analyte panels. Staining platform vendors currently encourage chromogenic mIHC panels for clinical application because of limited imaging and DIA platform availability in clinical labs and pathologist familiarity with chromogenic labeling. Advantages of fluorescence labeling include: 1) precise signal quantification; 2) increased sensitivity; 3) spectral channel separation; 4) standardization; 5) increased number of color options, and 6) facilitation of DIA.[243] Continued cost reductions in equipment and reagents will entice clinical labs to upgrade imaging and analytical capabilities. Care must be taken to ensure that mIHC panels are applied in a medically necessary way and subjected to standards and proficiency testing to be cognizant of patient costs.[244]

Conclusions

Our view of platforms “competing” with traditional and NGP histopathology is a welcoming one, especially during discovery and developmental phases because radiological, and -omics platforms are complementary. Computer hardware and software advances are driving a revolution in histopathology, which we have overviewed and illustrated its value. In our opinion, although fewer biopsies will likely be obtained, biopsies will be subjected to more intense scrutiny using NGP, which: 1) preserves spatial and inferred temporal contexts; 2) can rely on a worldwide distributed network of expert transplant pathophysiologists who, instead of relying on semiquantitative data rendering on biopsies, will have new toolkits that standardize objective quantitative output that limits or eliminates subjectivity and enhances reproducibility; and 3) engage various non-medical experts (eg, engineers, mathematicians, statisticians, and other biologists) into the realm of tissue analysis.

Integration of multiple data sources filtered through a variety of domain experts will provide a conceptual framework for scientific and patient care advancements. “Iterative loops” comparing morphometric, clinical, and -omics platforms data are informative and creative. Reliance on human input for morphology will continue, but software tools and ML will contribute to final biopsy interpretations once large WSI libraries are created and queried.

Author Manuscript Author Manuscript Author Manuscript Author Manuscript

Retention of spatial and inferred temporal context is essential because: 1) humans use visual inputs to conceptualize their environment; 2) it engages a worldwide network of expert mechanistic pathophysiologists who can interpret and develop in parallel -accelerating the rate of advancement; and 3) it retains software-based DIA and ML biopsy analyses. Until "grind and bind" or radiographic approaches discover methods to reconstruct the original spatial configuration from expression data or achieve the submicron spatial context resolution, respectively, both traditional histopathology and NGP are needed and will continue to be valued.

Supplementary Material

Refer to Web version on PubMed Central for supplementary material.

Acknowledgements

The authors thank the patients who agreed to participate in the clinical trials for which we serve as a core laboratory. The authors would also like to thank the following funding sources: Immune Tolerance Network (1UM1AI109565), Clinical Trials in Organ Transplantation in Children (1U01AI104336, 4U01AI104347), NIH/NAIAD (1U19AI131453, 4U01AI104347, U01AI100807), NIH/NIDDK (1R01DK114180), TransMedics, UPMC, and the Enduring Hearts Foundation.

ABBREVIATIONS:

AASLD	American Association for the Study of Liver Diseases
AMR	antibody-mediated rejection
APCs	antigen presenting cells
CAP	College of American Pathologists
CLIA	Clinical Laboratory Improvement Amendments
DIA	digital image analysis
CODEX	Co-detection by InDEXing
DSA	donor specific antigen
EMR	electronic medical record
FFPE	formalin-fixed, paraffin-embedded
H&E	hematoxylin and eosin
IHC	immunohistochemistry
IS	immunosuppression
ISH	in situ hybridization
IPEX	chromogenic immunohistochemistry
IVD	in vitro diagnostic

Author Manuscript Author Manuscript Author Manuscript Author Manuscript

mIHC	multiplex immunohistochemistry
ML	machine learning
LIMS	laboratory information management system
mRNA	messenger ribonucleic acid
NASH	nonalcoholic steatohepatitis
NBF	neutral buffered formalin
NGP	next generation pathology
NK cells	natural killer cells
PAS	periodic acid-Schiff
Qdots	quantum dots
QH	quantitative histomorphometry
RTU	ready to use
ROI	region of interest
TCMR	T cell-mediated rejection
TSA	tyramide signal amplification
TTC	tissue-tethered cytometry
USFDA	United States Food and Drug Administration
WSI	whole slide images

References

1. Jerath R, Crawford MW, Barnes VA. A unified 3D default space consciousness model combining neurological and physiological processes that underlie conscious experience. Front Psychol. 2015;6:1204. [PubMed: 26379573]
2. Romih T Humans Are Visual Creatures. https://www.seyens.com/humans-are-visual-creatures/. Accessed October 12, 2016.
3. Snyder A Explaining and inducing savant skills: privileged access to lower level, less-processed information. Philos Trans R Soc Lond B Biol Sci. 2009;364(1522):1399–1405. [PubMed: 19528023]
4. Khatri P, Sarwal MM. Using gene arrays in diagnosis of rejection. Curr Opin Organ Transplant. 2009;14(1):34–39. [PubMed: 19337144]
5. Isse K, Lesniak A, Grama K, Roysam B, Minervini MI, Demetris AJ. Digital transplantation pathology: combining whole slide imaging, multiplex staining and automated image analysis. Am J Transplant. 2012;12(1):27–37.
6. Kransdorf EP, Kobashigawa JA. Novel molecular approaches to the detection of heart transplant rejection. Per Med. 2017;14(4):293–297. [PubMed: 29749832]
7. Halloran PF, Famulski KS, Reeve J. Molecular assessment of disease states in kidney transplant biopsy samples. Nat Rev Nephrol. 2016;12(9):534–548. [PubMed: 27345248]

Author Manuscript Author Manuscript Author Manuscript Author Manuscript

8. Caussy C, Reeder SB, Sirlin CB, Loomba R. Noninvasive, quantitative assessment of liver fat by MRI-PDFF as an endpoint in NASH trials. Hepatology. 2018;68(2):763–772. [PubMed: 29356032]
9. Value English Oxford Living Dictionary. https://en.oxforddictionaries.com/definition/value. Oxford University Press; 2019 Accessed January 3, 2019.
10. Kennedy P, Wagner M, Castéra L, et al. Quantitative elastography methods in liver disease: current evidence and future directions. Radiology. 2018;286(3):738–763. [PubMed: 29461949]
11. Jiang H, Zheng T, Duan T, Chen J, Song B. Non-invasive in vivo imaging grading of liver fibrosis. J Clin Transl Hepatol. 2018;6(2):198–207. [PubMed: 29951365]
12. Wong GL. Non-invasive assessments for liver fibrosis: the crystal ball we long for. J Gastroenterol Hepatol. 2018;33(5):1009–1015. [PubMed: 29380413]
13. Tapper EB, Loomba R. Noninvasive imaging biomarker assessment of liver fibrosis by elastography in NAFLD. Nat Rev Gastroenterol Hepatol. 2018;15(5):274–282. [PubMed: 29463906]
14. Mancini M, Summers P, Faita F, et al. Digital liver biopsy: bio-imaging of fatty liver for translational and clinical research. World J Hepatol. 2018;10(2):231–245. [PubMed: 29527259]
15. Toby TK, Abecassis M, Kim K, et al. Proteoforms in peripheral blood mononuclear cells as novel rejection biomarkers in liver transplant recipients. Am J Transplant. 2017;17(9):2458–2467. [PubMed: 28510335]
16. Bonaccorsi-Riani E, Pennycuick A, Londono MC, et al. Molecular characterization of acute cellular rejection occurring during intentional immunosuppression withdrawal in liver transplantation. Am J Transplant. 2016;16(2):484–496. [PubMed: 26517400]
17. Khatri P, Roedder S, Kimura N, et al. A common rejection module (CRM) for acute rejection across multiple organs identifies novel therapeutics for organ transplantation. J Exp Med. 2013;210(11):2205–2221. [PubMed: 24127489]
18. Sigdel TK, Gao Y, He J, et al. Mining the human urine proteome for monitoring renal transplant injury. Kidney Int. 2016;89(6):1244–1252. [PubMed: 27165815]
19. Deng MC, Eisen HJ, Mehra MR, et al. Noninvasive discrimination of rejection in cardiac allograft recipients using gene expression profiling. Am J Transplant. 2006;6(1):150–160. [PubMed: 16433769]
20. Isse K, Grama K, Abbott IM, et al. Adding value to liver (and allograft) biopsy evaluation using a combination of multiplex quantum dot immunostaining, high-resolution whole-slide digital imaging, and automated image analysis. Clin Liver Dis. 2010;14(4):669–685. [PubMed: 21055689]
21. Patel K, Bedossa P, Castera L. Diagnosis of liver fibrosis: present and future. Semin Liver Dis. 2015;35(2):166–183. [PubMed: 25974902]
22. Vitalone MJ, Sigdel TK, Salomonis N, Sarwal RD, Hsieh SC, Sarwal MM. Transcriptional perturbations in graft rejection. Transplantation. 2015;99(9):1882–1893. [PubMed: 26154388]
23. Halloran PF, Venner JM, Madill-Thomsen KS, et al. Review: the transcripts associated with organ allograft rejection. Am J Transplant. 2018;18(4):785–795. [PubMed: 29178397]
24. Halloran PF, Potena L, Van Huyen JD, et al. Building a tissue-based molecular diagnostic system in heart transplant rejection: the heart Molecular Microscope Diagnostic (MMDx) System. J Heart Lung Transplant. 2017;36(11):1192–1200. [PubMed: 28662985]
25. Loupy A, Duong Van Huyen JP, Hidalgo L, et al. Gene expression profiling for the identification and classification of antibody-mediated heart rejection. Circulation. 2017;135(10):917–935. [PubMed: 28148598]
26. KASHI Clinical Laboratories. Molecular Microscope Diagnostic System (MMDx). https://www.molecular-microscope.com/clinicians. Accessed January 29, 2019.
27. Starzl TE, Marchioro TL, Terasaki PI, et al. Chronic survival after human renal homotransplantation. Lymphocyte-antigen matching, pathology and influence of thymectomy. Ann Surg. 1965;162(4):749–787. [PubMed: 5319400]
28. Kissmeyer-Nielsen F, Olsen S, Petersen VP, Fjeldborg O. Hyperacute rejection of kidney allografts, associated with pre-existing humoral antibodies against donor cells. Lancet. 1966;2(7465):662–665. [PubMed: 4162350]

Author Manuscript Author Manuscript Author Manuscript Author Manuscript

29. Ogden DA, Porter KA, Terasaki PI, Marchioro TL, Holmes JH, Starzl TE. Chronic renal homograft function: correlation with histology and lymphocyte antigen matching. Am J Med. 1967;43(6): 837–845. [PubMed: 4862761]
30. Porter KA, Dossetor JB, Marchioro TL, et al. Human renal transplants. I. Glomerular changes. Lab Invest. 1967;16(1):153–181. [PubMed: 5336793]
31. Porter KA. The effects of antibodies on human renal allografts. Transplant Proc. 1976;8(2):189–197.
32. Weil R 3rd, Clarke DR, Iwaki Y, et al. Hyperacute rejection of a transplanted human heart. Transplantation. 1981;32(1):71–72. [PubMed: 7022801]
33. Hancock WW. Analysis of intragraft effector mechanisms associated with human renal allograft rejection: immunohistological studies with monoclonal antibodies. Immunol Rev. 1984;77:61–84. [PubMed: 6232203]
34. Demetris AJ, Markus BH. Immunopathology of liver transplantation. Crit Rev Immunol. 1989;9(2):67–92. [PubMed: 2663025]
35. Hammond EH, Yowell RL, Nunoda S, et al. Vascular (humoral) rejection in heart transplantation: pathologic observations and clinical implications. J Heart Transplant. 1989;8(6):430–443. [PubMed: 2693662]
36. Halloran PF, Wadgymar A, Ritchie S, Falk J, Solez K, Srinivasa NS. The significance of the anti-class I antibody response. I. Clinical and pathologic features of anti-class I-mediated rejection. Transplantation. 1990;49(1):85–91. [PubMed: 2301035]
37. Halloran PF, Schlaut J, Solez K, Srinivasa NS. The significance of the anti-class I response. II. Clinical and pathologic features of renal transplants with anti-class I-like antibody. Transplantation. 1992;53(3):550–555. [PubMed: 1549846]
38. Demetris AJ, Murase N, Nakamura K, et al. Immunopathology of antibodies as effectors of orthotopic liver allograft rejection. [Review]. Semin Liver Dis. 1992;12(1):51–59. [PubMed: 1570551]
39. Lajoie G, Nadasdy T, Laszik Z, Blick KE, Silva FG. Mast cells in acute cellular rejection of human renal allografts. Mod Pathol. 1996;9(12):1118–1125. [PubMed: 8972470]
40. Racusen LC, Haas M. Antibody-mediated rejection in renal allografts: lessons from pathology. Clin J Am Soc Nephrol. 2006;1(3):415–420. [PubMed: 17699240]
41. Porter KA. Renal Transplantation In: Heptinstall RH, ed. Pathology of the Kidney. Vol III 4th ed. Boston/Toronto/London: Little, Brown and Company; 1992:1799–1934.
42. Halloran PF, de Freitas DG, Einecke G, et al. The molecular phenotype of kidney transplants. Am J Transplant. 2010;10(10):2215–2222. [PubMed: 20931695]
43. Drachenberg CB, Papadimitriou JC. Endothelial injury in renal antibody-mediated allograft rejection: a schematic view based on pathogenesis. Transplantation. 2013;95(9):1073–1083. [PubMed: 23370711]
44. Karlsson C, Karlsson MG. Effects of long-term storage on the detection of proteins, DNA, and mRNA in tissue microarray slides. J Histochem Cytochem. 2011;59(12):1113–1121. [PubMed: 22147608]
45. Reeve J, Chang J, Salazar ID, Lopez MM, Halloran PF. Using molecular phenotyping to guide improvements in the histologic diagnosis of T cell-mediated rejection. Am J Transplant. 2016;16(4):1183–1192. [PubMed: 26730747]
46. Roufosse C, Simmonds N, Groningen MC, et al. A 2018 reference guide to the banff classification of renal allograft pathology. Transplantation. 2018;102(11):1795–1814. [PubMed: 30028786]
47. Rockey DC, Caldwell SH, Goodman ZD, Nelson RC, Smith AD. Liver biopsy. Hepatology. 2009;49(3):1017–1044. [PubMed: 19243014]
48. Pandey N, John S. Liver Biopsy [1 2018 ed]. In: StatPearls.Treasure Island, FL: StatPearls Publishing; 2018.
49. Feng S, Ekong UD, Lobritto SJ, et al. Complete immunosuppression withdrawal and subsequent allograft function among pediatric recipients of parental living donor liver transplants. JAMA. 2012;307(3):283–293. [PubMed: 22253395]

Author Manuscript Author Manuscript Author Manuscript Author Manuscript

50. Zheng J, Song W. Alemtuzumab versus antithymocyte globulin induction therapies in kidney transplantation patients: a systematic review and meta-analysis of randomized controlled trials. Medicine (Baltimore). 2017;96(28):e7151. [PubMed: 28700465]
51. Haas M, Loupy A, Lefaucheur C, et al. The Banff 2017 Kidney Meeting Report: revised diagnostic criteria for chronic active T cell-mediated rejection, antibody-mediated rejection, and prospects for integrative endpoints for next-generation clinical trials. Am J Transplant. 2018;18(2):293–307. [PubMed: 29243394]
52. Bedossa P Diagnosis of non-alcoholic fatty liver disease/non-alcoholic steatohepatitis: why liver biopsy is essential. Liver Int. 2018;38 Suppl 1:64–66. [PubMed: 29427497]
53. Rodríguez-Perálvarez M, Rico-Juri JM, Tsochatzis E, Burra P, De la Mata M, Lerut J. Biopsy-proven acute cellular rejection as an efficacy endpoint of randomized trials in liver transplantation: a systematic review and critical appraisal. Transpl Int. 2016;29(9):961–973. [PubMed: 26714264]
54. Williams J FDA regulatory considerations for NASH clinical trial endpoints Global NASH Congress; 2018; London, UK.
55. Demetris AJ, Bellamy C, Hubscher SG, et al. 2016 comprehensive update of the Banff Working Group on liver allograft pathology: introduction of antibody-mediated rejection. Am J Transplant. 2016;16(10):2816–2835. [PubMed: 27273869]
56. O'Leary JG, Smith C, Cai J, et al. Chronic AMR in liver transplant: validation of the 1-year cAMR score's ability to determine long-term outcome. Transplantation. 2017;101(9):2062–2070. [PubMed: 28452922]
57. O'Leary JG, Cai J, Freeman R, et al. Proposed diagnostic criteria for chronic antibody-mediated rejection in liver allografts. Am J Transplant. 2016;16(2):603–614. [PubMed: 26469278]
58. O'Leary JG, Kaneku H, Demetris AJ, et al. Antibody-mediated rejection as a contributor to previously unexplained early liver allograft loss. Liver Transpl. 2014;20(2):218–227. [PubMed: 24382837]
59. O'Leary JG, Michelle Shiller S, Bellamy C, et al. Acute liver allograft antibody-mediated rejection: an inter-institutional study of significant histopathological features. Liver Transpl. 2014;20(10):1244–1255. [PubMed: 25045154]
60. Feng S, Bucuvalas JC, Demetris AJ, et al. Evidence of chronic allograft injury in liver biopsies from long-term pediatric recipients of liver transplants. Gastroenterology. 2018;155(6):1838–1851. [PubMed: 30144432]
61. Feng S, Demetris AJ, Spain KM, et al. Five-year histological and serological follow-up of operationally tolerant pediatric liver transplant recipients enrolled in WISP-R. Hepatology. 2017;65(2):647–660. [PubMed: 27302659]
62. Barisoni L, Troost JP, Nast C, et al. Reproducibility of the NEPTUNE descriptor-based scoring system on whole-slide images and histologic and ultrastructural digital images. Mod Pathol. 2016;29(7):671–684. [PubMed: 27102348]
63. Snyder A, Bahramali H, Hawker T, Mitchell DJ. Savant-like numerosity skills revealed in normal people by magnetic pulses. Perception. 2006;35(6):837–845. [PubMed: 16836048]
64. Mells G, Neuberger J. Protocol liver allograft biopsies. Transplantation. 2008;85(12):1686–1692. [PubMed: 18580457]
65. Mells G, Mann C, Hubscher S, Neuberger J. Late protocol liver biopsies in the liver allograft: a neglected investigation? Liver Transpl. 2009;15(8):931–938. [PubMed: 19642126]
66. Russo FP, Imondi A, Lynch EN, Farinati F. When and how should we perform a biopsy for HCC in patients with liver cirrhosis in 2018? A review. Dig Liver Dis. 2018;50(7):640–646. [PubMed: 29636240]
67. Brunt EM. Nonalcoholic fatty liver disease and the ongoing role of liver biopsy evaluation. Hepatol Commun. 2017;1(5):370–378. [PubMed: 29404465]
68. Gill US, Pallett LJ, Kennedy PTF, Maini MK. Liver sampling: a vital window into HBV pathogenesis on the path to functional cure. Gut. 2018;67(4):767–775. [PubMed: 29331944]
69. Mieli-Vergani G, Vergani D, Czaja AJ, et al. Autoimmune hepatitis. Nat Rev Dis Primers. 2018;4:18017. [PubMed: 29644994]

Author Manuscript Author Manuscript Author Manuscript Author Manuscript

70. Londoño MC, Souza LN, Lozano JJ, et al. Molecular profiling of subclinical inflammatory lesions in long-term surviving adult liver transplant recipients. J Hepatol. 2018;69(3):626–634. [PubMed: 29709679]
71. Baumann AK, Schlue J, Noyan F, et al. Preferential accumulation of T helper cells but not cytotoxic T cells characterizes benign subclinical rejection of human liver allografts. Liver Transpl. 2016;22(7):943–955. [PubMed: 26929119]
72. Demetris AJ, Isse K. Tissue biopsy monitoring of operational tolerance in liver allograft recipients. Curr Opin Organ Transplant. 2013;18(3):345–353. [PubMed: 23619515]
73. Hubscher SG. What is the long-term outcome of the liver allograft? Journal of Hepatology. 2011;55(3):702–717. [PubMed: 21426919]
74. Hubscher S What does the long-term liver allograft look like for the pediatric recipient? Liver Transpl. 2009;15 Suppl 2:S19–S24. [PubMed: 19877293]
75. Demetris AJ, Jaffe R, Sheahan DG, et al. Recurrent hepatitis B in liver allograft recipients. Differentiation between viral hepatitis B and rejection. Am J Pathol. 1986;125(1):161–172. [PubMed: 3535528]
76. Demetris AJ, Jaffe R, Tzakis A, et al. Antibody-mediated rejection of human orthotopic liver allografts. A study of liver transplantation across ABO blood group barriers. Am J Pathol. 1988;132(3):489–502. [PubMed: 3046369]
77. Demetris AJ, Nakamura K, Yagihashi A, et al. A clinicopathological study of human liver allograft recipients harboring preformed IgG lymphocytotoxic antibodies. Hepatology. 1992;16(3):671–681. [PubMed: 1505910]
78. Demetris AJ, Eghtesad B, Marcos A, et al. Recurrent hepatitis C in liver allografts: prospective assessment of diagnostic accuracy, identification of pitfalls, and observations about pathogenesis. Am J Surg Pathol. 2004;28(5):658–669. [PubMed: 15105656]
79. O'Leary JG, Demetris AJ, Friedman LS, et al. The role of donor-specific HLA alloantibodies in liver transplantation. Am J Transplant. 2014;14(4):779–787. [PubMed: 24580828]
80. O'Leary JG, Demetris AJ, Philippe A, et al. Non-HLA antibodies impact on C4d staining, stellate cell activation and fibrosis in liver allografts. Transplantation. 2017;101(10):2399–2409. [PubMed: 28665894]
81. Varma S, Ambroise J, Komuta M, et al. Progressive fibrosis is driven by genetic predisposition, allo-immunity, and inflammation in pediatric liver transplant recipients. EBioMedicine. 2016;9:346–355. [PubMed: 27333038]
82. Demetris AJ, Zeevi A, O'Leary JG. ABO-compatible liver allograft antibody-mediated rejection: an update. Curr Opin Organ Transplant. 2015;20(3):314–324. [PubMed: 25944231]
83. Miyagawa-Hayashino A, Yoshizawa A, Uchida Y, et al. Progressive graft fibrosis and donor-specific human leukocyte antigen antibodies in pediatric late liver allografts. Liver Transpl. 2012;18(11):1333–1342. [PubMed: 22888064]
84. Banff Working Group on Liver Allograft Pathology. Importance of liver biopsy findings in immunosuppression management: biopsy monitoring and working criteria for patients with operational tolerance. Liver Transpl. 2012;18(10):1154–1170. [PubMed: 22645090]
85. Wong T, Nouri-Aria KT, Devlin J, Portmann B, Williams R. Tolerance and latent cellular rejection in long-term liver transplant recipients. Hepatology. 1998;28(2):443–449. [PubMed: 9696010]
86. Kerkar N, Yanni G. 'De novo' and 'recurrent' autoimmune hepatitis after liver transplantation: A comprehensive review. J Autoimmun. 2016;66:17–24. [PubMed: 26377632]
87. Solez K, Fung KC, Saliba KA, et al. The bridge between transplantation and regenerative medicine: beginning a new Banff classification of tissue engineering pathology. Am J Transplant. 2018;18(2):321–327. [PubMed: 29194964]
88. Stack EC, Wang C, Roman KA, Hoyt CC. Multiplexed immunohistochemistry, imaging, and quantitation: a review, with an assessment of Tyramide signal amplification, multispectral imaging and multiplex analysis. Methods. 2014;70(1):46–58. [PubMed: 25242720]
89. Dixon AR, Bathany C, Tsuei M, White J, Barald KF, Takayama S. Recent developments in multiplexing techniques for immunohistochemistry. Expert Rev Mol Diagn. 2015;15(9):1171–1186. [PubMed: 26289603]

Author Manuscript Author Manuscript Author Manuscript Author Manuscript

90. Mansfield JR. Phenotyping multiple subsets of immune cells in situ in FFPE tissue sections: an overview of methodologies. Methods Mol Biol. 2017;1546:75–99. [PubMed: 27896758]
91. Kim SW, Roh J, Park CS. Immunohistochemistry for pathologists: protocols, pitfalls, and tips. J Pathol Transl Med. 2016;50(6):411–418. [PubMed: 27809448]
92. Taylor CR. Immunohistochemistry in surgical pathology: principles and practice. Methods Mol Biol. 2014;1180:81–109. [PubMed: 25015143]
93. Demetris AJ, Ruppert K. Pathologist's perspective on liver needle biopsy size? J Hepatol. 2003;39(2):275–277. [PubMed: 12873827]
94. Piccinino F, Sagnelli E, Pasquale G, Giusti G. Complications following percutaneous liver biopsy. A multicentre retrospective study on 68,276 biopsies. J Hepatol. 1986;2(2):165–173. [PubMed: 3958472]
95. Atwell TD, Smith RL, Hesley GK, et al. Incidence of bleeding after 15,181 percutaneous biopsies and the role of aspirin. AJR Am J Roentgenol. 2010;194(3):784–789. [PubMed: 20173160]
96. Tublin ME, Blair R, Martin J, Malik S, Ruppert K, Demetris A. Prospective study of the impact of liver biopsy core size on specimen adequacy and procedural complications. AJR Am J Roentgenol. 2018;210(1):183–188. [PubMed: 29091001]
97. Tublin ME, Blair R, Martin JA, Ruppert K, Demetris A. RC614–03 Ultrasound Guided Random Liver Biopsy: Impact of Biopsy Core Size on Specimen Adequacy and Procedural Complications Paper presented at: Radiological Society of North America 2015 Scientific Assembly and Annual Meeting; Chicago, IL.
98. Iqbal J, Sattar A, Al Qamari N, Hussain M, Rashid S. Compare the efficacy and complications of 16 gauge vs 18 gauge core biopsy needle in ultrasound guided percutaneous liver biopsies. J Dow Uni Health Sci. 2017;11(2):37–40.
99. Hall TC, Deakin C, Atwal GS, Singh RK. Adequacy of percutaneous non-targeted liver biopsy under real-time ultrasound guidance when comparing the Biopince™ and Achieve™ biopsy needle. Br J Radiol. 2017;90(1080):20170397. [PubMed: 28972801]
100. Myers RP, Fong A, Shaheen AA. Utilization rates, complications and costs of percutaneous liver biopsy: a population-based study including 4275 biopsies. Liver Int. 2008;28(5):705–712. [PubMed: 18433397]
101. Filingeri V, Sforza D, Tisone G. Complications and risk factors of a large series of percutaneous liver biopsies in patients with liver transplantation or liver disease. Eur Rev Med Pharmacol Sci. 2015;19(9):1621–1629. [PubMed: 26004602]
102. Nicholson ML, Wheatley TJ, Doughman TM, et al. A prospective randomized trial of three different sizes of core-cutting needle for renal transplant biopsy. Kidney Int. 2000;58(1):390–395. [PubMed: 10886586]
103. Smith RN, Adam BA, Rosales IA, et al. RNA expression profiling of renal allografts in a nonhuman primate identifies variation in NK and endothelial gene expression. Am J Transplant. 2018;18(6):1340–1350. [PubMed: 29286578]
104. Fitzgibbons PL, Bradley LA, Fatheree LA, et al. Principles of analytic validation of immunohistochemical assays: Guideline from the College of American Pathologists Pathology and Laboratory Quality Center. Arch Pathol Lab Med. 2014;138(11):1432–1443. [PubMed: 24646069]
105. Wolff AC, Hammond ME, Hicks DG, et al. Recommendations for human epidermal growth factor receptor 2 testing in breast cancer: American Society of Clinical Oncology/College of American Pathologists clinical practice guideline update. J Clin Oncol. 2013;31(31):3997–4013. [PubMed: 24101045]
106. Wolff AC, Hammond MEH, Allison KH, et al. Human epidermal growth factor receptor 2 testing in breast cancer: American Society of Clinical Oncology/College of American Pathologists Clinical Practice guideline focused update. J Clin Oncol. 2018;36(20):2105–2122. [PubMed: 29846122]
107. Hammond ME, Hayes DF, Dowsett M, et al. American Society of Clinical Oncology/College Of American Pathologists guideline recommendations for immunohistochemical testing of estrogen and progesterone receptors in breast cancer. J Clin Oncol. 2010;28(16):2784–2795. [PubMed: 20404251]

Author Manuscript Author Manuscript Author Manuscript Author Manuscript

108. Economou M, Schöni L, Hammer C, Galván JA, Mueller DE, Zlobec I. Proper paraffin slide storage is crucial for translational research projects involving immunohistochemistry stains. Clin Transl Med. 2014;3(1):4. [PubMed: 24636624]
109. Bass BP, Engel KB, Greytak SR, Moore HM. A review of preanalytical factors affecting molecular, protein, and morphological analysis of formalin-fixed, paraffin-embedded (FFPE) tissue: how well do you know your FFPE specimen? Arch Pathol Lab Med. 2014;138(11):1520–1530. [PubMed: 25357115]
110. Lott R, Tunnicliffe J, Sheppard E, et al. Practical Guide to Specimen Handling in Surgical Pathology. 6th ed: College of American Pathologists; 11 2015.
111. Pinhel IF, Macneill FA, Hills MJ, et al. Extreme loss of immunoreactive p-Akt and p-Erk1/2 during routine fixation of primary breast cancer. Breast Cancer Res. 2010;12(5):R76. [PubMed: 20920193]
112. Neumeister VM, Anagnostou V, Siddiqui S, et al. Quantitative assessment of effect of preanalytic cold ischemic time on protein expression in breast cancer tissues. J Natl Cancer Inst. 2012;104(23):1815–1824. [PubMed: 23090068]
113. Aziz N, Zhao Q, Bry L, et al. College of American Pathologists' laboratory standards for next-generation sequencing clinical tests. Arch Pathol Lab Med. 2015;139(4):481–493. [PubMed: 25152313]
114. Endrullat C, Glökler J, Franke P, Frohme M. Standardization and quality management in next-generation sequencing. Appl Transl Genom. 2016;10:2–9. [PubMed: 27668169]
115. Macedo C, Walters JT, Orkis EA, et al. Long-term effects of alemtuzumab on regulatory and memory T-cell subsets in kidney transplantation. Transplantation. 2012;93(8):813–821. [PubMed: 22343334]
116. Corbitt N, Kimura S, Isse K, et al. Gut bacteria drive Kupffer cell expansion via MAMP-mediated ICAM-1 induction on sinusoidal endothelium and influence preservation-reperfusion injury after orthotopic liver transplantation. Am J Pathol. 2013;182(1):180–191. [PubMed: 23159949]
117. Feng S, Demetris AJ, Ekong U, et al. Serum and Tissue DSA Subclass, Stellate and Endothelial Phenotype Monitoring in ITN029ST Tolerance Pediatric Liver Transplant Recipients Over 5+ Years of Follow-up. Joint International Conference of ILTS, ELITA & LICAGE; June 4–7, 2014; London, UK.
118. Isse K, Specht SM, Lunz JG 3rd, Kang LI, Mizuguchi Y, Demetris AJ. Estrogen stimulates female biliary epithelial cell interleukin-6 expression in mice and humans. Hepatology. 2010;51(3):869–880. [PubMed: 20043322]
119. Isse K, Lesniak A, Grama K, et al. Preexisting epithelial diversity in normal human livers: a tissue-tethered cytometric analysis in portal/periportal epithelial cells. Hepatology. 2013;57(4):1632–1643. [PubMed: 23150208]
120. Mizuguchi Y, Isse K, Specht S, et al. Small proline rich protein 2a in benign and malignant liver disease. Hepatology. 2014;59(3):1130–1143. [PubMed: 24123265]
121. Mizuguchi Y, Specht S, Isse K, et al. Breast tumor kinase/protein tyrosine kinase 6 (Brk/PTK6) activity in normal and neoplastic biliary epithelia. J Hepatol. 2015;63(2):399–407. [PubMed: 25770659]
122. Feng Z, Puri S, Moudgil T, et al. Multispectral imaging of formalin-fixed tissue predicts ability to generate tumor-infiltrating lymphocytes from melanoma. J Immunother Cancer. 2015;3:47. [PubMed: 26500776]
123. Zhang W, Hubbard A, Jones T, et al. Fully automated 5-plex fluorescent immunohistochemistry with tyramide signal amplification and same species antibodies. Lab Invest. 2017;97(7):873–885. [PubMed: 28504684]
124. Mezheyeuski A, Bergsland CH, Backman M, et al. Multispectral imaging for quantitative and compartment-specific immune infiltrates reveals distinct immune profiles that classify lung cancer patients. J Pathol. 2018;244(4):421–431. [PubMed: 29282718]
125. Ng SB, Fan S, Choo SN, et al. Quantitative analysis of a multiplexed immunofluorescence panel in T-cell lymphoma. SLAS Technol. 2018;23(3):252–258. [PubMed: 29241019]

Author Manuscript Author Manuscript Author Manuscript Author Manuscript

126. Hu Z, Qian G, Müller S, et al. Biomarker quantification by multiplexed quantum dot technology for predicting lymph node metastasis and prognosis in head and neck cancer. Oncotarget. 2016;7(28):44676–44685. [PubMed: 27172790]

127. Kauffman SA. The Origins of Order: Self Organization and Selection in Evolution. New York: Oxford University Press; 1993.

128. NanoString Technologies Inc. Digital Spatial Profiling (DSP) Technology. https://www.nanostring.com/scientific-content/technology-overview/digital-spatial-profiling-technology. Accessed June 15, 2018.

129. Thul PJ, Åkesson L, Wiking M, et al. A subcellular map of the human proteome. Science. 2017;356(6340):eaal3321. [PubMed: 28495876]

130. Uhlén M, Fagerberg L, Hallström BM, et al. Proteomics. Tissue-based map of the human proteome. Science. 2015;347(6220):1260419. [PubMed: 25613900]

131. Uhlen M, Zhang C, Lee S, et al. A pathology atlas of the human cancer transcriptome. Science. 2017;357(6352):eaan2507. [PubMed: 28818916]

132. Abcam plc. Substrates and chromogens for IHC. https://www.abcam.com/kits/substrates-and-chromogens-for-ihc. Accessed July 2, 2018.

133. Shi SR, Shi Y, Taylor CR. Antigen retrieval immunohistochemistry: review and future prospects in research and diagnosis over two decades. J Histochem Cytochem. 2011;59(1):13–32. [PubMed: 21339172]

134. Shi SR, Liu C, Taylor CR. Standardization of immunohistochemistry for formalin-fixed, paraffin-embedded tissue sections based on the antigen-retrieval technique: from experiments to hypothesis. J Histochem Cytochem. 2007;55(2):105–109. [PubMed: 16982846]

135. Hunyady B, Krempels K, Harta G, Mezey E. Immunohistochemical signal amplification by catalyzed reporter deposition and its application in double immunostaining. J Histochem Cytochem. 1996;44(12):1353–1362. [PubMed: 8985127]

136. Tóth ZE, Mezey E. Simultaneous visualization of multiple antigens with tyramide signal amplification using antibodies from the same species. J Histochem Cytochem. 2007;55(6):545–554. [PubMed: 17242468]

137. Hagen J, Schwartz D, Kalyuzhny AE. Hapten-anti-hapten technique for two-color IHC detection of phosphorylated EGFR and H2AX using primary antibodies raised in the same host species. Methods Mol Biol. 2017;1554:155–160. [PubMed: 28185188]

138. Angelo M, Bendall SC, Finck R, et al. Multiplexed ion beam imaging of human breast tumors. Nat Med. 2014;20(4):436–442. [PubMed: 24584119]

139. Rost S, Giltnane J, Bordeaux JM, Hitzman C, Koeppen H, Liu SD. Multiplexed ion beam imaging analysis for quantitation of protein expression in cancer tissue sections. Lab Invest. 2017;97(8):992–1003. [PubMed: 28553935]

140. Goltsev Y, Samusik N, Kennedy-Darling J, et al. Deep profiling of mouse splenic architecture with CODEX multiplexed imaging. Cell. 2018;174(4):968–981.e915. [PubMed: 30078711]

141. Trahearn N, Epstein D, Cree I, Snead D, Rajpoot N. Hyper-stain inspector: a framework for robust registration and localised co-expression analysis of multiple whole-slide images of serial histology sections. Sci Rep. 2017;7(1):5641. [PubMed: 28717124]

142. Lopez XM, Barbot P, Van Eycke YR, et al. Registration of whole immunohistochemical slide images: an efficient way to characterize biomarker colocalization. J Am Med Inform Assoc. 2015;22(1):86–99. [PubMed: 25125687]

143. Vorob'ev IA, Rafalovskaia-Orlovskaia EP, Gladkikh AA, Potashnikova DM, Barteneva NS. [Applications of fluorescent semiconductor nanocrystals in microscopy and cytometry]. Tsitologiia. 2011;53(5):392–403. [PubMed: 21786682]

144. Prost S, Kishen RE, Kluth DC, Bellamy CO. Working with commercially available quantum dots for immunofluorescence on tissue sections. PLoS One. 2016;11(9):e0163856. [PubMed: 27685858]

145. Zhang W, Hubbard A, Pang L, et al. Protecting quantum dot fluorescence from quenching to achieve a reliable automated multiplex fluorescence in situ hybridization assay. J Biomed Nanotechnol. 2015;11(9):1583–1596. [PubMed: 26485928]

Author Manuscript Author Manuscript Author Manuscript Author Manuscript

146. Day WA, Lefever MR, Ochs RL, et al. Covalently deposited dyes: a new chromogen paradigm that facilitates analysis of multiple biomarkers in situ. Lab Invest. 2017;97(1):104–113. [PubMed: 27869794]

147. van Gijlswijk RP, Zijlmans HJ, Wiegant J, et al. Fluorochrome-labeled tyramides: use in immunocytochemistry and fluorescence in situ hybridization. J Histochem Cytochem. 1997;45(3):375–382. [PubMed: 9071319]

148. Pirici D, Mogoanta L, Kumar-Singh S, et al. Antibody elution method for multiple immunohistochemistry on primary antibodies raised in the same species and of the same subtype. J Histochem Cytochem. 2009;57(6):567–575. [PubMed: 19223296]

149. Boyce BF. An update on the validation of whole slide imaging systems following FDA approval of a system for a routine pathology diagnostic service in the United States. Biotech Histochem. 2017;92(6):381–389. [PubMed: 28836859]

150. Parwani AV, Hassell L, Glassy E, Pantanowitz L. Regulatory barriers surrounding the use of whole slide imaging in the United States of America. J Pathol Inform. 2014;5(1):38. [PubMed: 25379344]

151. Cornish TC, Swapp RE, Kaplan KJ. Whole-slide imaging: routine pathologic diagnosis. Adv Anat Pathol. 2012;19(3):152–159. [PubMed: 22498580]

152. Hartman DJ, Pantanowitz L, McHugh JS, Piccoli AL, OLeary MJ, Lauro GR. Enterprise implementation of digital pathology: feasibility, challenges, and opportunities. J Digit Imaging. 2017;30(5):555–560. [PubMed: 28116576]

153. Evans AJ, Salama ME, Henricks WH, Pantanowitz L. Implementation of whole slide imaging for clinical purposes: issues to consider from the perspective of early adopters. Arch Pathol Lab Med. 2017;141(7):944–959. [PubMed: 28440660]

154. Pantanowitz L Digital images and the future of digital pathology. J Pathol Inform. 2010;1:15. [PubMed: 20922032]

155. Pantanowitz L, Valenstein PN, Evans AJ, et al. Review of the current state of whole slide imaging in pathology. J Pathol Inform. 2011;2:36. [PubMed: 21886892]

156. Pantanowitz L, Sinard JH, Henricks WH, et al. Validating whole slide imaging for diagnostic purposes in pathology: guideline from the College of American Pathologists Pathology and Laboratory Quality Center. Arch Pathol Lab Med. 2013;137(12):1710–1722. [PubMed: 23634907]

157. Cross S, Furness P, Igali L, Snead D, Treanor D. Best practice recommendations for implementing digital pathology. The Royal College of Pathologists. https://www.rcpath.org/uploads/assets/uploaded/d6b14330-a8b9-4f5e-bbe443f0d56de24a.pdf. Accessed January 29, 2019.

158. Brown JR, Wimberly H, Lannin DR, Nixon C, Rimm DL, Bossuyt V. Multiplexed quantitative analysis of CD3, CD8, and CD20 predicts response to neoadjuvant chemotherapy in breast cancer. Clin Cancer Res. 2014;20(23):5995–6005. [PubMed: 25255793]

159. Caccomo S FDA allows marketing of first whole slide imaging system for digital pathology. https://www.fda.gov/NewsEvents/Newsroom/PressAnnouncements/ucm552742.htm. Accessed July 15, 2018.

160. Fasciano D, Pavlidakey P. 298 Digital pathology cost effective – fact or fiction? Am J Clin Pathol. 2018;149(Suppl 1):S126–S127.

161. Langbein W Smaller Labs Eyeing Digital Pathology as Options Grow. https://www.360dx.com/clinical-lab-management/smaller-labs-eyeing-digital-pathology-options-grow. Accessed April 23, 2018.

162. Shaw EC, Hanby AM, Wheeler K, et al. Observer agreement comparing the use of virtual slides with glass slides in the pathology review component of the POSH breast cancer cohort study. J Clin Pathol. 2012;65(5):403–408. [PubMed: 22447915]

163. Mukhopadhyay S, Feldman MD, Abels E, et al. Whole slide imaging versus microscopy for primary diagnosis in surgical pathology: a multicenter blinded randomized noninferiority study of 1992 cases (pivotal study). Am J Surg Pathol. 2018;42(1):39–52. [PubMed: 28961557]

Author Manuscript Author Manuscript Author Manuscript Author Manuscript

164. Bauer TW, Schoenfield L, Slaw RJ, Yerian L, Sun Z, Henricks WH. Validation of whole slide imaging for primary diagnosis in surgical pathology. Arch Pathol Lab Med. 2013;137(4):518–524. [PubMed: 23323732]
165. Słodkowska J, Pankowski J, Siemiatkowska K, Chyczewski L. Use of the virtual slide and the dynamic real-time telepathology systems for a consultation and the frozen section intra-operative diagnosis in thoracic/pulmonary pathology. Folia Histochem Cytobiol. 2009;47(4):679–684. [PubMed: 20430738]
166. Saco A, Diaz A, Hernandez M, et al. Validation of whole-slide imaging in the primary diagnosis of liver biopsies in a University Hospital. Dig Liver Dis. 2017;49(11):1240–1246. [PubMed: 28780052]
167. ThermoFisher Scientific. Molecular Probes™ Handbook: A Guide to Fluorescent Probes and Labeling Technologies. https://www.thermofisher.com/us/en/home/references/molecular-probes-the-handbook/introduction-to-fluorescence-techniques.html. Accessed July 8, 2018.
168. Beier HT, Ibey BL. Experimental comparison of the high-speed imaging performance of an EM-CCD and sCMOS camera in a dynamic live-cell imaging test case. PLoS One. 2014;9(1):e84614. [PubMed: 24404178]
169. Park KS, Kim DU, Lee J, Kim GH, Chang KS. Simultaneous multicolor imaging of wide-field epi-fluorescence microscopy with four-bucket detection. Biomed Opt Express. 2016;7(6):2285–2294. [PubMed: 27375944]
170. Fu X, Lennerz JK, Onozato M, Iafrate A, Yagi Y. Evaluation of a confocal WSI scanner for FISH slide imaging and image analysis. Diagn Pathol. 2017;3:249.
171. Liao J, Bian L, Bian Z, et al. Single-frame rapid autofocusing for brightfield and fluorescence whole slide imaging. Biomed Opt Express. 2016;7(11):4763–4768. [PubMed: 27896014]
172. Loussert Fonta C, Humbel BM. Correlative microscopy. Arch Biochem Biophys. 2015;581:98–110. [PubMed: 26072116]
173. Feingold B, Picarsic J, Lesniak A, Popp BA, Wood-Trageser MA, Demetris AJ. Late graft dysfunction after pediatric heart transplantation is associated with fibrosis and microvasculopathy by automated, digital whole-slide analysis. J Heart Lung Transplant. 2017;36(12):1336–1343. [PubMed: 29055602]
174. Blom S, Paavolainen L, Bychkov D, et al. Systems pathology by multiplexed immunohistochemistry and whole-slide digital image analysis. Sci Rep. 2017;7(1):15580. [PubMed: 29138507]
175. Christiansen EM, Yang SJ, Ando DM, et al. In silico labeling: predicting fluorescent labels in unlabeled images. Cell. 2018;173(3):792–803.e719. [PubMed: 29656897]
176. Bautista PA, Yagi Y. Improving the visualization and detection of tissue folds in whole slide images through color enhancement. J Pathol Inform. 2010;1:25. [PubMed: 21221170]
177. Kothari S, Phan JH, Wang MD. Eliminating tissue-fold artifacts in histopathological whole-slide images for improved image-based prediction of cancer grade. J Pathol Inform. 2013;4:22. [PubMed: 24083057]
178. Lopez XM, D'Andrea E, Barbot P, et al. An automated blur detection method for histological whole slide imaging. PLoS One. 2013;8(12):e82710. [PubMed: 24349343]
179. Campanella G, Rajanna AR, Corsale L, Schüffler PJ, Yagi Y, Fuchs TJ. Towards machine learned quality control: a benchmark for sharpness quantification in digital pathology. Comput Med Imaging Graph. 2018;65:142–151. [PubMed: 29241972]
180. Jen KY, Olson JL, Brodsky S, Zhou XJ, Nadasdy T, Laszik ZG. Reliability of whole slide images as a diagnostic modality for renal allograft biopsies. Hum Pathol. 2013;44(5):888–894. [PubMed: 23199528]
181. Ozluk Y, Blanco PL, Mengel M, Solez K, Halloran PF, Sis B. Superiority of virtual microscopy versus light microscopy in transplantation pathology. Clin Transplant. 2012;26(2):336–344. [PubMed: 21955102]
182. Al-Janabi S, Huisman A, Jonges GN, Ten Kate FJ, Goldschmeding R, van Diest PJ. Whole slide images for primary diagnostics of urinary system pathology: a feasibility study. J Renal Inj Prev. 2014;3(4):91–96. [PubMed: 25610886]

Author Manuscript Author Manuscript Author Manuscript Author Manuscript

183. Brazdziute E, Laurinavicius A. Digital pathology evaluation of complement C4d component deposition in the kidney allograft biopsies is a useful tool to improve reproducibility of the scoring. Diagn Pathol. 2011;6 Suppl 1: S5. [PubMed: 21489200]

184. Neil DAH, Bellamy CO, Smith M, et al. Global quality assessment of liver allograft C4d staining during acute antibody-mediated rejection in formalin-fixed, paraffin-embedded tissue. Hum Pathol. 2018;73:144–155. [PubMed: 29288041]

185. Daunoravicius D, Besusparis J, Zurauskas E, et al. Quantification of myocardial fibrosis by digital image analysis and interactive stereology. Diagn Pathol. 2014;9:114. [PubMed: 24912374]

186. Fu R, Ma X, Bian Z, Ma J. Digital separation of diaminobenzidine-stained tissues via an automatic color-filtering for immunohistochemical quantification. Biomed Opt Express. 2015;6(2):544–558. [PubMed: 25780744]

187. Isgro G, Calvaruso V, Andreana L, et al. The relationship between transient elastography and histological collagen proportionate area for assessing fibrosis in chronic viral hepatitis. J Gastroenterol. 2013;48(8):921–929. [PubMed: 23124603]

188. Manousou P, Burroughs AK, Tsochatzis E, et al. Digital image analysis of collagen assessment of progression of fibrosis in recurrent HCV after liver transplantation. J Hepatol. 2013;58(5):962–968. [PubMed: 23262247]

189. Calvaruso V, Dhillon AP, Tsochatzis E, et al. Liver collagen proportionate area predicts decompensation in patients with recurrent hepatitis C virus cirrhosis after liver transplantation. J Gastroenterol Hepatol. 2012;27(7):1227–1232. [PubMed: 22432427]

190. Manousou P, Dhillon AP, Isgro G, et al. Digital image analysis of liver collagen predicts clinical outcome of recurrent hepatitis C virus 1 year after liver transplantation. Liver Transpl. 2011;17(2):178–188. [PubMed: 21280191]

191. Calvaruso V, Burroughs AK, Standish R, et al. Computer-assisted image analysis of liver collagen: relationship to Ishak scoring and hepatic venous pressure gradient. Hepatology. 2009;49(4):1236–1244. [PubMed: 19133646]

192. Diaz Encarnacion MM, Griffin MD, Slezak JM, et al. Correlation of quantitative digital image analysis with the glomerular filtration rate in chronic allograft nephropathy. Am J Transplant. 2004;4(2):248–256. [PubMed: 14974947]

193. Servais A, Meas-Yedid V, Buchler M, et al. Quantification of interstitial fibrosis by image analysis on routine renal biopsy in patients receiving cyclosporine. Transplantation. 2007;84(12): 1595–1601. [PubMed: 18165770]

194. Meas-Yedid V, Servais A, Noël LH, et al. New computerized color image analysis for the quantification of interstitial fibrosis in renal transplantation. Transplantation. 2011;92(8):890–899. [PubMed: 21926945]

195. Farris AB, Adams CD, Brousaides N, et al. Morphometric and visual evaluation of fibrosis in renal biopsies. J Am Soc Nephrol. 2011;22(1):176–186. [PubMed: 21115619]

196. Farris AB, Chan S, Climenhaga J, et al. Banff fibrosis study: multicenter visual assessment and computerized analysis of interstitial fibrosis in kidney biopsies. Am J Transplant. 2014;14(4): 897–907. [PubMed: 24712330]

197. Pickering JG, Boughner DR. Fibrosis in the transplanted heart and its relation to donor ischemic time. Assessment with polarized light microscopy and digital image analysis. Circulation. 1990;81(3):949–958. [PubMed: 2306841]

198. Lerut E, Kuypers DR, Verbeken E, et al. Acute rejection in non-compliant renal allograft recipients: a distinct morphology. Clin Transplant. 2007;21(3):344–351. [PubMed: 17488383]

199. Bräsen JH, Khalifa A, Schmitz J, et al. Macrophage density in early surveillance biopsies predicts future renal transplant function. Kidney Int. 2017;92(2):479–489. [PubMed: 28359537]

200. Moon A, Smith GH, Kong J, Rogers TE, Ellis CL, Farris ABB. Development of CD3 cell quantitation algorithms for renal allograft biopsy rejection assessment utilizing open source image analysis software. Virchows Arch. 2018;472(2):259–269. [PubMed: 29116389]

201. Sorrentino C, Scarinci A, D'Antuono T, et al. Endomyocardial infiltration by B and NK cells foreshadows the recurrence of cardiac allograft rejection. J Pathol. 2006;209(3):400–410. [PubMed: 16583358]

Author Manuscript Author Manuscript Author Manuscript Author Manuscript

202. El-Badry AM, Breitenstein S, Jochum W, et al. Assessment of hepatic steatosis by expert pathologists: the end of a gold standard. Ann Surg. 2009;250(5):691–697. [PubMed: 19806055]
203. Hall AR, Dhillon AP, Green AC, et al. Hepatic steatosis estimated microscopically versus digital image analysis. Liver Int. 2013;33(6): 926–935. [PubMed: 23560780]
204. Vertemati M, Petrella D, Gambacorta M, Bonacina E, Vizzotto L. Predictive value of computerized morphometric analysis of steatosis in donor livers. Anal Quant Cytopathol Histpathol. 2014;36(3): 137–146. [PubMed: 25141490]
205. Reis H, Peterek PT, Wohlschlaeger J, et al. Oil Red O-assessed macrosteatosis in liver transplant donor biopsies predicts ischemia-reperfusion injury and clinical outcome. Virchows Arch. 2014;464(2):165–174. [PubMed: 24297629]
206. Lauronen J, Häyry P, Paavonen T. An image analysis-based method for quantification of chronic allograft damage index parameters. APMIS. 2006;114(6):440–448. [PubMed: 16856966]
207. Moccia S, Mattos LS, Patrini I, et al. Computer-assisted liver graft steatosis assessment via learning-based texture analysis. Int J Comput Assist Radiol Surg. 2018;13(9):1357–1367. [PubMed: 29796834]
208. Goodman ZD, Becker RL Jr., Pockros PJ, Afdhal NH. Progression of fibrosis in advanced chronic hepatitis C: evaluation by morphometric image analysis. Hepatology. 2007;45(4):886–894. [PubMed: 17393526]
209. Huang Y, de Boer WB, Adams LA, MacQuillan G, Bulsara MK, Jeffrey GP. Image analysis of liver biopsy samples measures fibrosis and predicts clinical outcome. J Hepatol. 2014;61(1):22–27. [PubMed: 24607623]
210. Irshad H, Veillard A, Roux L, Racoceanu D. Methods for nuclei detection, segmentation, and classification in digital histopathology: a review-current status and future potential. IEEE Rev Biomed Eng. 2014;7:97–114. [PubMed: 24802905]
211. Denic A, Alexander MP, Kaushik V, et al. Detection and clinical patterns of nephron hypertrophy and nephrosclerosis among apparently healthy adults. Am J Kidney Dis. 2016;68(1):58–67. [PubMed: 26857648]
212. Klapczynski M, Gagne GD, Morgan SJ, et al. Computer-assisted imaging algorithms facilitate histomorphometric quantification of kidney damage in rodent renal failure models. J Pathol Inform. 2012;3:20. [PubMed: 22616032]
213. Abe T, Hashiguchi A, Yamazaki K, et al. Quantification of collagen and elastic fibers using whole-slide images of liver biopsy specimens. Pathol Int. 2013;63(6):305–310. [PubMed: 23782332]
214. Castillo-Rama M, Sebagh M, Sasatomi E, et al. “Plasma Cell Hepatitis” in Liver Allografts: Identification and Characterization of an IgG4-Rich Cohort. Am J Transplant. 2013;13(11):2966–2977. [PubMed: 24011021]
215. Mizuguchi Y, Specht S, Lunz JG 3rd, et al. SPRR2a enhances p53 deacetylation through HDAC1 and down regulates p21 promoter activity. BMC Mol Biol. 2012;13:20. [PubMed: 22731250]
216. Serón D, Moreso F. Protocol biopsies in renal transplantation: prognostic value of structural monitoring. Kidney Int. 2007;72(6):690–697. [PubMed: 17597702]
217. Madabhushi A, Lee G. Image analysis and machine learning in digital pathology: Challenges and opportunities. Med Image Anal. 2016;33:170–175. [PubMed: 27423409]
218. Sharma H, Zerbe N, Lohmann S, Kayser K, Hellwich O, Hufnagl P. A review of graph-based methods for image analysis in digital histopathology. Diagn Pathol. 2015;1(2015):61.
219. Bhatia AK, Phan JH, Kothari S, Shehata B, Wang M. Automated analysis of histopathological whole slide images to diagnose pediatric heart transplant rejection. J Heart Lung Transplant. 2015;34(4):S327.
220. Kayser K, Görtler J, Borkenfeld S, Kayser G. How to measure diagnosis-associated information in virtual slides. Diagn Pathol. 2011;6 Suppl 1:S9. [PubMed: 21489204]
221. Riber-Hansen R, Vainer B, Steiniche T. Digital image analysis: a review of reproducibility, stability and basic requirements for optimal results. APMIS. 2012;120(4):276–289. [PubMed: 22429210]

Author Manuscript Author Manuscript Author Manuscript Author Manuscript

222. Wan S, Zhao E, Kryczek I, et al. Tumor-associated macrophages produce interleukin 6 and signal via STAT3 to promote expansion of human hepatocellular carcinoma stem cells. Gastroenterology. 2014;147(6):1393–1404. [PubMed: 25181692]

223. Yoshida N, Kinugasa T, Miyoshi H, et al. A high RORγT/CD3 ratio is a strong prognostic factor for postoperative survival in advanced colorectal cancer: analysis of helper T cell lymphocytes (Th1, Th2, Th17 and regulatory T cells). Ann Surg Oncol. 2016;23(3):919–927. [PubMed: 26564244]

224. Abadjian MZ, Edwards WB, Anderson CJ. Imaging the tumor microenvironment. Adv Exp Med Biol. 2017;1036:229–257. [PubMed: 29275475]

225. Saltz J, Gupta R, Hou L, et al. Spatial organization and molecular correlation of tumor-infiltrating lymphocytes using deep learning on pathology images. Cell Rep. 2018;23(1):181–193.e187. [PubMed: 29617659]

226. Djuric U, Zadeh G, Aldape K, Diamandis P. Precision histology: how deep learning is poised to revitalize histomorphology for personalized cancer care. NPJ Precis Oncol. 2017;1(1):22. [PubMed: 29872706]

227. Jordan MI, Mitchell TM. Machine learning: trends, perspectives, and prospects. Science. 2015;349(6245):255–260. [PubMed: 26185243]

228. Li Z, Zhang X, Müller H, Zhang S. Large-scale retrieval for medical image analytics: a comprehensive review. Med Image Anal. 2018;43:66–84. [PubMed: 29031831]

229. Zheng Y, Jiang Z, Zhang H, et al. Histopathological whole slide image analysis using context-based CBIR. IEEE Trans Med Imaging. 2018;37(7):1641–1652. [PubMed: 29969415]

230. Janowczyk A, Madabhushi A. Deep learning for digital pathology image analysis: a comprehensive tutorial with selected use cases. J Pathol Inform. 2016;7:29. [PubMed: 27563488]

231. Sirinukunwattana K, Ahmed Raza SE, Tsang Yee-Wah, Snead DR, Cree IA, Rajpoot NM. Locality sensitive deep learning for detection and classification of nuclei in routine colon cancer histology images. IEEE Trans Med Imaging. 2016;35(5):1196–1206. [PubMed: 26863654]

232. Mobadersany P, Yousefi S, Amgad M, et al. Predicting cancer outcomes from histology and genomics using convolutional networks. Proc Natl Acad Sci USA. 2018;115(13):E2970–E2979. [PubMed: 29531073]

233. Holzinger A Interactive machine learning for health informatics: when do we need the human-in-the-loop? Brain Inform. 2016;3(2):119–131. [PubMed: 27747607]

234. Samek W, Binder A, Montavon G, Lapuschkin S, Muller KR. Evaluating the Visualization of What a Deep Neural Network Has Learned. IEEE Trans Neural Netw Learn Syst. 2017;28(11): 2660–2673. [PubMed: 27576267]

235. DICOM Standards Committee Working Group 26 Pathology. Digital Imaging and Communications in Medicine (DICOM) Supplement 145: Whole Slide Microscopic Image IOD and SOP Classes. ftp://medical.nema.org/medical/dicom/final/sup145_ft.pdf Accessed July 2, 2018.

236. Goode A, Gilbert B, Harkes J, Jukic D, Satyanarayanan M. OpenSlide: a vendor-neutral software foundation for digital pathology. J Pathol Inform. 2013;4:27. [PubMed: 24244884]

237. Bankhead P, Loughrey MB, Fernández JA, et al. QuPath: open source software for digital pathology image analysis. Sci Rep. 2017;7(1):16878. [PubMed: 29203879]

238. Williams E, Moore J, Li SW, et al. The Image Data Resource: a bioimage data integration and publication platform. Nat Methods. 2017;14(8):775–781. [PubMed: 28775673]

239. Gutman DA, Khalilia M, Lee S, et al. The Digital Slide Archive: a software platform for management, integration, and analysis of histology for cancer research. Cancer Res. 2017;77(21):e75–e78. [PubMed: 29092945]

240. Wang F, Oh TW, Vergara-Niedermayr C, Kurc T, Saltz J. Managing and querying whole slide images. Proc SPIE Int Soc Opt Eng. 2012;8319:pii 83190J.

241. Wang F, Kong J, Cooper L, et al. A data model and database for high-resolution pathology analytical image informatics. J Pathol Inform. 2011;2:32. [PubMed: 21845230]

242. Fraggetta F, Garozzo S, Zannoni GF, Pantanowitz L, Rossi ED. Routine digital pathology workflow: the Catania experience. J Pathol Inform. 2017;8:51. [PubMed: 29416914]

Author Manuscript Author Manuscript Author Manuscript Author Manuscript

243. Gaigalas AK, Li L, Henderson O, et al. The development of fluorescence intensity standards. J Res Natl Inst Stand Technol. 2001;106(2):381–389. [PubMed: 27500028]

244. Yaziji H, Eisen R, Wick M, et al. Immunohistochemistry cocktails are here to stay: Center for Medicare and Medicaid Services should revise its new reimbursement policy. Am J Clin Pathol. 2012;138(1):10–11. [PubMed: 22706851]

245. Im M, Chae H, Kim T, et al. Comparative quantitative analysis of cluster of differentiation 45 antigen expression on lymphocyte subsets. Korean J Lab Med. 2011;31(3):148–153. [PubMed: 21779186]

246. McGuinness PH, Painter D, Davies S, McCaughan GW. Increases in intrahepatic CD68 positive cells, MAC387 positive cells, and proinflammatory cytokines (particularly interleukin 18) in chronic hepatitis C infection. Gut. 2000;46(2):260–269. [PubMed: 10644323]

247. Huang R, Wu H, Liu Y, et al. Increase of infiltrating monocytes in the livers of patients with chronic liver diseases. Discov Med. 2016;21(113):25–33. [PubMed: 26896599]

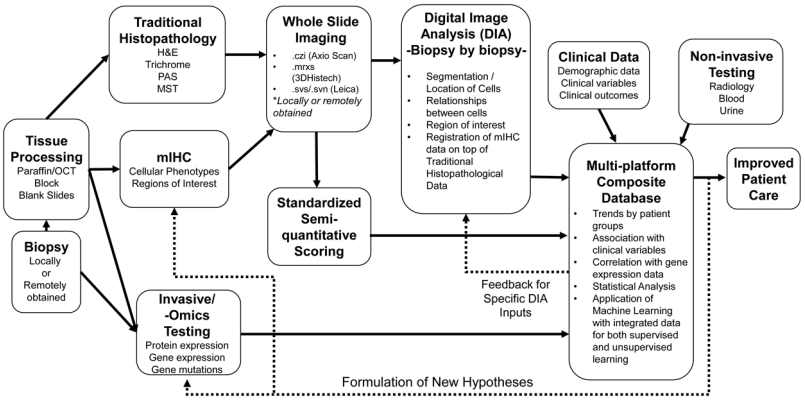


Figure 1.

Overall workflow and NGP integration with other data sources. Locally- or remotely obtained tissue biopsies can be triaged for traditional and NGP and tissue shared with other “invasive” non-histopathology platforms either before or after FFPE processing. WSI can be created at the core laboratory or electronically transferred from remote sites thus saving repeat traditional histochemical staining and preserving tissue for other NGP assays. NGP-generated data can then be integrated with clinical and serological data, noninvasive imaging and fluid -omics and invasive tissue-based -omics platforms for analysis. Dashed lines indicate iterative processes where feedback from a later stage is incorporated to optimize a result.

Author Manuscript Author Manuscript Author Manuscript Author Manuscript

Author Manuscript Author Manuscript Author Manuscript Author Manuscript

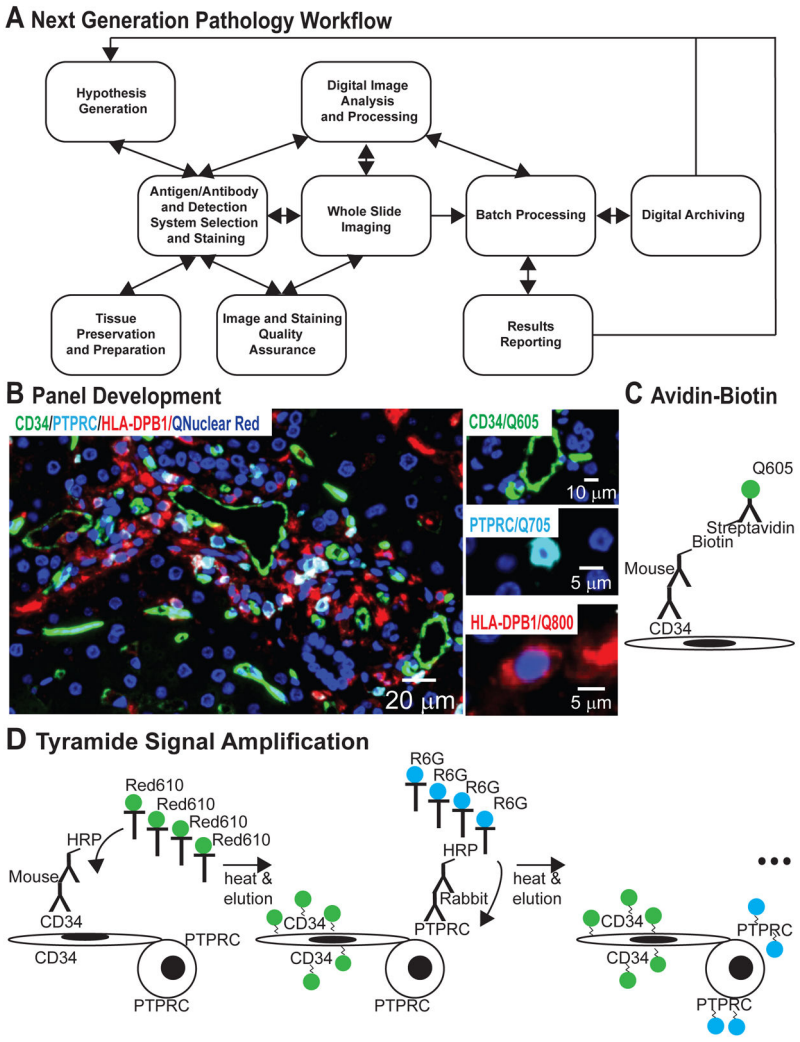


Figure 2.

Next generation pathology workflow and initial panel development. (A) NGP requires hypothesis generation, potential antigenic targets, available antibodies, and preferred detection systems. Tissue preservation and preparation should facilitate staining. Analytics occur simultaneously and iteratively with panel development, scanning optimization, and QA; each step providing feedback to others. Samples are then batch processed using the same protocol/metrics for each sample without human intervention culminating in objective data reporting and archiving. (B) The CD34/PTPRC/HLA-DPB1 multiplex IHC panel: CD34 (green) labels elongated endothelial cells lining the portal microvasculature. PTPRC^{high} (cyan) mostly labels lymphocytes[245] resulting in circular, cytoplasmic “donut”. HLA-DPB1 (red) can appear on any antigen presenting cell (ie, oddly shaped macrophages, round PTPRC positive B cells, and dendritic and endothelial cells). The larger image shows an overlay of all labeled antigens with nuclei shown in blue. See Table S1 for sample workflow details. (C) Avidin-biotin amplification systems are used for sequential detection of proteins via primary antibodies from the same host species (eg, detection of CD34). (D) Tyramide signal amplification systems are used for sequential detection of primary

Author Manuscript Author Manuscript Author Manuscript Author Manuscript

antibodies from the same or different host species. The catalyst horseradish peroxidase activates tyramide-conjugated fluorophores causing them to covalently bind to protein tyrosine residues near the target antigen. Covalent binding enables heat deactivation, denaturation, and elution of primary and secondary antibodies leaving the fluorophore covalently bound to the target antigen and facilitating subsequent staining steps.

Author Manuscript Author Manuscript Author Manuscript Author Manuscript

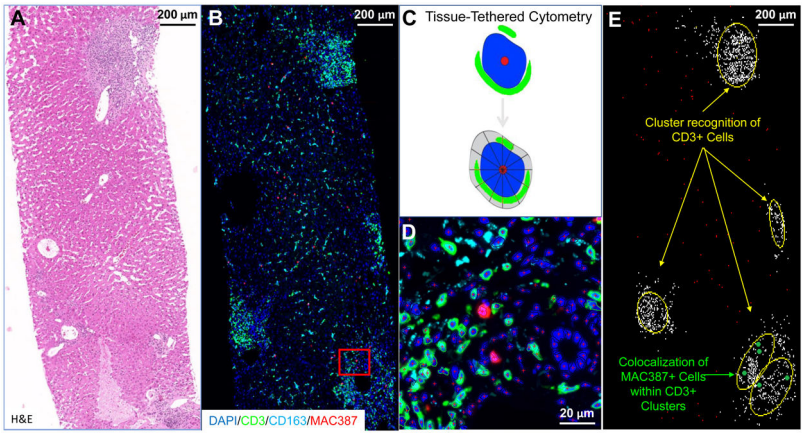


Figure 3.

An example of objective quantitative analysis of replacing semiquantitative scoring. (A) An H&E image of a biopsy with obvious portal lymphocytic inflammation (top right) would be scored semi-quantitatively as mild to moderate portal inflammation. The lymphocyte phenotypes and quantitative analysis of each cell type are undiscernible from this traditionally stained and scoring approach. However, human only analysis can be improved by mIHC staining and automated DIA. (B) For example, CD3(green)/MAC387(red)/CD163(cyan) panel can be used to detect and quantify total T cells (CD3) and recent monocyte/macrophage immigrants (MAC387) signaling some type of liver injury,[246,247] and resident Kupffer cells (CD163). The red box identifies the high-power field shown in D. (C) A combination of pixel-based and QH can identify individual cells and their phenotypic characteristics based on analyte expression, which can be used to objectively report the total number of each cell type per mm^2 of biopsy area or in certain tissue areas (eg, portal tracts). Here we localize nuclear (blue) or cytoplasmic (green) analytes in possible identified cytoplasmic regions (grey) per segmented nucleus. (D) The number of cells matching the criteria defined in C are then indicated by Nearcyte, a hand-crafted" tissue-tethered cytometric software and can be quantified. (E) An unsupervised clustering algorithm can be used to identify and highlight abnormal "clustering" of $CD3^+$ T cells using objective computational algorithms, such as mixed gaussian models (yellow ovals). The proximity to and type of APC present in these clusters, like $MAC387^+$ or $CD163^+$ cells, can be analyzed to determine whether recent immigrants or liver-based, possibly more tolerogenic, cells, respectively, are interacting with tissue-based $CD3^+$ cells. $MAC387^+$ cells are indicated with green dots.

Author Manuscript Author Manuscript Author Manuscript Author Manuscript

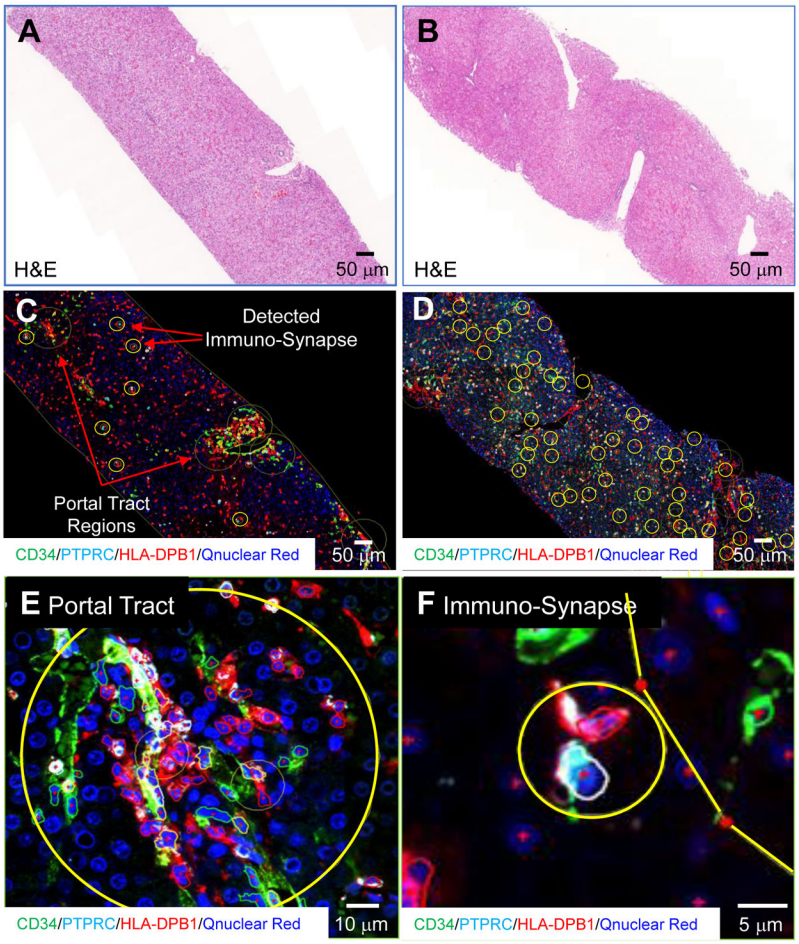


Figure 4.

Digital image analysis. (A) and (B) are from two patients at time 0 (before attempted IS weaning). Overall the severity of the negligible portal and lobular inflammation is similar based on analysis of the H&E-stained sections. However, when the same biopsies (C) and (D), respectively, are mIHC stained for CD34 (green), PTPRC (cyan), HLA-DPB1 (red), and QNuclear Deep Red stain (blue) the stark difference between the two is easily recognizable. (C) DIA to identify pairings (virtual immunological synapses) between APC and PTPRC+ cells (yellow circles) highlights a vast difference between the two biopsies that is not recognizable on the H&E stains. Note the noticeable difference between (C) and (D) that is not noticeable on the H&E stains. (E) DIA is also able to recognize portal tract regions defined as a 100 μm radius zone centered on 5 or more HLA-DPB1+ (red) cells within a 25 μm area (large thin yellow circles). (F) DIA is able to identify “virtual immunological synapses” formed between two cells that may not be apparent to the human eye, in this case a $CD34^{-}/PTPRC^{-}/HLA\text{-}DPB1^{+}$ (red) cell within 5 μm of a $CD34^{-}/PTPRC^{+}/HLA\text{-}DPB1^{+}$ (leukocyte) cell (small thick yellow circles). Quantitation of these features can be queried and combined with spatial information to infer relationships about antigen presenting cells in portal tracts.

Author Manuscript Author Manuscript Author Manuscript Author Manuscript

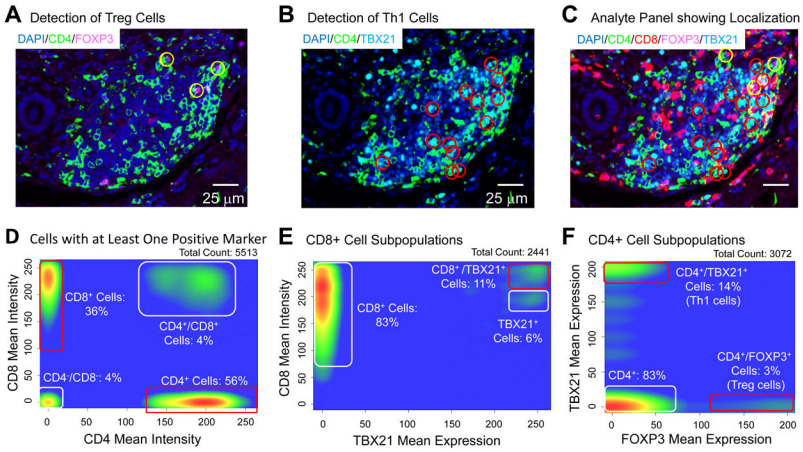


Figure 5.

Multidimensional morphometric data generation and tissue-tethered cytometry. DIA can dissect tissue cell populations and produce data outputs mimicking flow cytometry, while maintaining the spatial context of mIHC panels. Automated detection of tissue area, nuclear segmentation, and analyte expression/cell are performed via NearCYTE. This mIHC panel included CD4 (green), CD8 (red), FOXP3 (magenta), TBX21 (cyan), and nuclei (blue) to help characterize different T cell phenotypes. (A–F) Cellular subpopulations can be graphically represented on the mIHC-stained tissue sections: (A; $CD4^+/FOXP3^+$ cells; yellow circles) and (B; $CD4^+/TBX21^+$ cells; red circles). (C) Overlay of all mIHC panel components with DIA can be used to quantify cell types and inform relationships among cell types and tissue structures. Morphometric data, maintaining spatial relationships between cell types, can be translated into a traditional flow plot with the color intensity representative of the percentage of cells (green less cell density to red more cell density). (D) Cell plot representing $CD4^+$ versus $CD8^+$ cells from all cells that had at least one mIHC panel label. (E) $CD8^+$ cells were queried for subpopulations expressing TBX21. (F) $CD4^+$ cells were queried for subpopulations into putative Tregs expressing FOXP3 or Th1 cells expressing TBX21.

Author Manuscript Author Manuscript Author Manuscript Author Manuscript

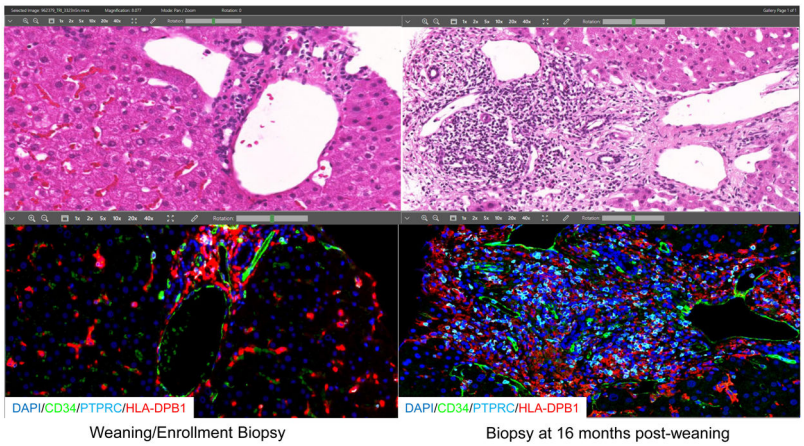


Figure 6.

Vendor-neutral web-based viewing solution. This vendor-neutral viewing platform enables direct side-by-side comparisons of biopsies from the same patient at two different time points. The “Weaning/Enrollment Biopsy” (left) and “Biopsy at 16 months post-weaning (right) show representative portal tracts from H&E-stained (top row) and CD34/HLA-DPB1^{+}/PTPRC^{high} stained mIHC panel (bottom row). Quantitative queries, analyses, and mechanistic insights can be carried out with respect to treatment changes between the two timepoints. This platform also enables receipt of WSI created elsewhere thus eliminating the need to repeat common stains (H&E, PAS, trichrome, etc) preserving tissue for other analyses.